Intestinal toxicity of the new type A trichothecenes, NX and 3ANX

Alix Pierron, Manon Neves, Sylvie Puel, Yannick Lippi, Laura Soler-Vasco, J. David Miller, Isabelle P. Oswald

Intestinal toxicity of the new type A trichothecenes, NX and 3ANX

Alix Pierron[1*], Manon Neves[1*], Sylvie Puel[1], Yannick Lippi[1], Laura Soler[1], J. David Miller[2] and Isabelle P. Oswald[1]

[1] *Toxalim (Research Center in Food Toxicology), Université de Toulouse, INRA, ENVT, INP-Purpan, Toulouse, France*

[2] *Department of Chemistry, Carleton University, 1125 Colonel By Drive, Ottawa, Ontario K1S 5B6, Canada*

**These authors contributed equally to this work*

Corresponding Author:

Isabelle P. Oswald PhD

INRA, UMR-1331, Toxalim, 180 chemin de Tournefeuille, 31027 Toulouse cedex 3, France

Phone +33 582066366

E-Mail: Isabelle.Oswald@inrae.fr

Intestinal toxicity of the new discovered type A trichothecenes, NX and 3ANX

Highlights:

- Differential cytotoxicity in human Caco-2 cells: NX=DON>3ANX
- Number of differentially expressed genes in intestinal explant NX>>DON>3ANX
- NX, 3ANX and DON modulate pathways mainly related to inflammation and immune response

Intestinal toxicity of the new discovered type A trichothecenes, NX and 3ANX

Graphical abstract:

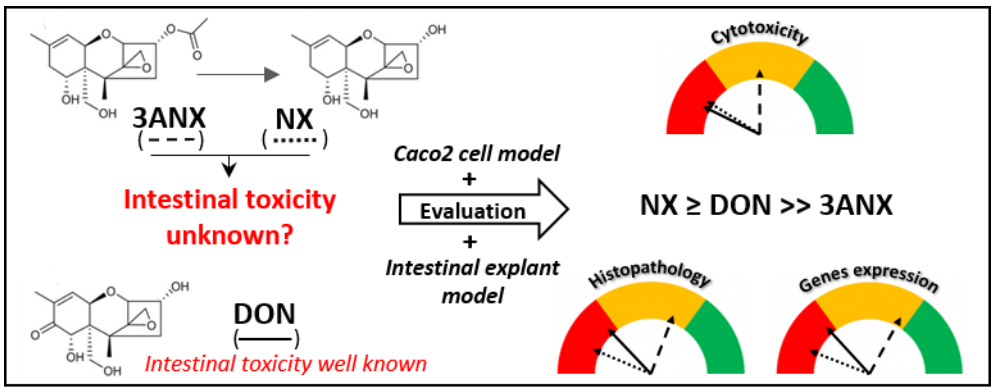

Abstract

NX and its acetylated form 3ANX are two new type A trichothecenes produced by *Fusarium graminearum* whose toxicity is poorly documented. The aim of this study was to obtain a general view of the intestinal toxicity of these toxins. Deoxynivalenol (DON), which differs from NX by the keto group at C8, served as a benchmark. The viability of human intestinal Caco-2 cells decreased after 24 h of exposure to 3 µM NX (-21.4%), 3 µM DON (-20.2%) or 10 µM 3ANX (-17.4%). Histological observations in porcine jejunal explants exposed for 4 h to 10 µM of the different toxins showed interstitial edema and cellular debris. Explants exposed to NX also displayed cell vacuolization, a broken epithelial barrier and high loss of villi. Whole transcriptome profiling revealed that NX, DON and 3ANX modulated 369, 146 and 55 genes, respectively. Functional analyses indicated that the three toxins regulate the same gene networks and signaling pathways mainly; cell proliferation, differentiation, apoptosis and growth, and particularly immune and pro-inflammatory responses. Greater transcriptional impacts were observed with NX than with DON. In conclusion, our data revealed that the three toxins have similar impacts on the intestine but of different magnitude: NX > DON >> 3ANX. NX and 3ANX should consequently be included in overall risk analysis linked to the presence of trichothecenes in our diet.

Keywords: deoxynivalenol, gut, *Fusarium graminearum,* explant, transcriptome

1. Introduction

Mycotoxins are toxic secondary metabolites produced by various filamentous fungi including *Aspergillus, Penicillium* and *Fusarium*. A number of compounds –notably *Fusarium graminearum* metabolites deoxynivalenol (DON) and zearalenone– are common contaminants of wheat and corn in temperate regions worldwide (Miller 2016). In Europe, Asia and North America, exposure to the *F. graminearum* trichothecene DON plus its two acetylates and its glucosides derivatives can approach or exceed tolerable daily intakes, especially in children (JEFCA, 2011; Knutsen et al., 2017; Vin et al., 2020).

There have been changes in the distribution and genetics of *F. graminearum* populations in different parts of the world including the appearance of two new chemotypes (Crippin et al., 2019). Gale et al. (2010) discovered a population of *F. graminearum* in the Midwest United States that was genotyped as 3ADON but did not produce 3ADON, 15ADON, DON, fusarenone X, or nivalenol. Closer investigation of these strains determined that this population produced new trichothecenes, one of which was similar to 3ADON but lacked C-8 keto oxygen. This compound was given the trivial name 3ANX (also called NX-2) and its deacetylated form, NX (also called NX-3) (Aitken et al., 2019; Varga et al., 2015). This population has subsequently been detected elsewhere around the Great Lakes. Working with a population collected in an area of more than 20,000 km^2 in southern Ontario, Crippin et al. found another new population within the 15ADON genotype that produced both 15ADON and 3ANX (Crippin et al., 2020, 2019). Analyses of grain samples that contained high amounts of DON also revealed NX at 1- 7% of the DON concentration (Crippin et al., 2020).

DON is one of the most widely studied mycotoxins and has many effects including on protein synthesis, immune system function, impact on the intestine and interactions with several appetite suppression systems. It is regulated based on the basis of its anorexic effect (JEFCA, 2011; Knutsen et al., 2017; Pestka, 2010). DON interacts with the peptidyl transferase region of the 60S ribosomal subunit. It triggers ribotoxic stress resulting in the activation of mitogen-activated protein kinases (MAPKs) and causes apoptosis and inflammation (Garreau de Loubresse et al., 2014; Payros et al., 2016; Pestka, 2010). Oxidative stress is also known to play a role in DON-induced toxicity (Da Silva et al., 2018; You et al., 2021). In humans, acute exposure to DON is associated with vomiting and bloody diarrhea (Ruan

et al., 2020) while chronic exposure leads to reduced food consumption and reduced weight gain, neuro-endocrine changes as well as alteration of immune functions (Payros et al., 2016; Pestka, 2010; Robert et al., 2017). In contrast, toxicological characterization of NX and 3ANX is limited but the few data available suggest similarities with DON. Like DON, NX is cytotoxic to mammalian cancer and non-cancer cell lines, inhibits protein synthesis, increases the intracellular concentration of ROS and has a pro-inflammatory effect (Varga et al., 2018, 2015; Woelflingseder et al., 2020, 2018).

The intestine is the first barrier against food born chemical contaminants, including mycotoxins (Pierron et al., 2016c). The gastrointestinal tract is particularly impacted by DON, as this mycotoxin alters intestinal morphology, impairs barrier function and nutrient absorption (Ghareeb et al., 2015; Pierron et al., 2016a; Pinton and Oswald, 2014). DON also triggers intestinal inflammation, which could increase susceptibility to intestinal inflammatory diseases (Maresca et al., 2008; Payros et al., 2020; Pestka, 2010).

This paper had two objectives. The first one was to obtain a general view of the toxicological alterations of the intestine induced by the new toxins NX and 3ANX in comparison to the one of DON. This was possible thanks to the use of the Caco-2 cell line and intestinal porcine explants. The second objective was to rank these three toxins for their intestinal toxicity based on cytotoxicity, histopathological analysis and whole transcriptome profiling. These data will increase our understanding the toxicity of the new toxins NX and 3ANX and benefit the safety assessment of mycotoxin as agricultural contaminants.

2. Material and Methods

2.1. Toxins

Deoxynivalenol (DON) was purchased from Sigma-Aldrich (St. Quentin Fallavier, France). 3ANX (type-A trichothecene 7a-hydroxy, 15-deacetylcalonectrin) and NX (deacetylated product 7a-hydroxy, 3, 15-dideacetylcalonectrin) were produced following the methods described in Aitken et al. (2019). The three toxins were dissolved in purified water and were aliquoted at a stock concentration of 5 mM at -20°C. The chemical structure of the three toxins is displayed in Suppl. Fig.1.

97 2.2. Caco-2 cell culture and viability assay

98 Caco-2 cells obtained from Sigma-Aldrich (passage 69-71, Acc n°86010202) were cultured as
99 previously described (Luo et al., 2021). Briefly, Caco-2 cells were cultured in 75-cm^2 culture flasks in
100 Dulbecco's Modified Eagle Medium (Gibco, Life Technologies, Courtaboeuf, France) enriched with
101 1% L-glutamine (862 mg/L) and supplemented with 10% of heat inactivated fetal bovine serum
102 (Eurobio, Courtaboeuf, France), 0.5% of Gentamycin (Eurobio) and 1% of MEM non-essential amino
103 acids (L-alanine (890 mg/L), L-asparagine (1500 mg/L), L-aspartic acid (1330 mg/L), L-glycine (750
104 mg/L), L-serine (1050 mg/L), L-proline (1150 mg/L) and L-glutamic acid (1470 mg/L)) (M7145,
105 Sigma-Aldrich). Cells were maintained at 37 °C in 5% CO_2 atmosphere and 90% relative humidity and
106 passaged by trypsinization (0.5% trypsin in 0.5 mM EDTA, Eurobio) when they reached 80% of
107 confluency. Cell viability was assayed with the CellTiter-Glo Luminescent Cell Viability Assay
108 (Promega, Charbonnières-les-Bains, France) according to manufacturer's instructions. Cells were
109 seeded at a density of 1.56×10^5 cells/cm^2 in 96-well microtiter white plates with clear bottom (Greiner).
110 Cells were grown for 24 h and exposed to DON, NX or 3ANX at different concentrations (0.03-100
111 µM), for 24 or 48 h. Luminescence was measured with a spectrophotometer (TECAN Spark, Männedorf,
112 Switzerland).
113
114 2.3. Jejunum explant culture

115 A total of 11 4-week-old crossbred castrated male piglets were used. The experiment was conducted
116 under the guidelines of the French Ministry of Agriculture for animal research. All animal
117 experimentation procedures were approved by the Ethics Committee of Pharmacology-Toxicology of
118 Toulouse-Midi-Pyrénées in animal experimentation (Toxcométhique) (N°: TOXCOM/0163/PP) in
119 accordance with the European Directive on the protection of animals used for scientific purposes
120 (Directive 2010/63/EU). Jejunal explants were obtained as previously described (García et al., 2018).
121 The explants were incubated 30 minutes in complete control medium, William's Medium E (Sigma-
122 Aldrich), Glucose 4.5 g/L (Sigma-Aldrich), ITS (Insulin Transferrin Sodium selenite) 1X (Sigma-
123 Aldrich), Alanyl-Glutamine 30 mM (Sigma-Aldrich), Penicillin-Streptomycin 1% and Gentamycin
124 0.5% (Eurobio). Then, treated in complete medium with toxins, for 4 h at 39 °C with 10 µM of DON,

NX or 3ANX, conditions already described (Alassane-Kpembi et al., 2017; Pinton et al., 2012). After incubation, the explants were fixed in formalin or snap frozen in liquid nitrogen and stored at −80 °C.

2.4. Histological analysis

Explants fixed with 10% formalin (Sigma-Aldrich) for 24 h were dehydrated and embedded in paraffin wax (Labonord, Templemars, France) using standard histological procedures. Sections (5-µm-thick) were stained with hematoxylin and eosin (Sigma-Aldrich) for histopathological assessment as previously described (Alassane-Kpembi et al., 2017). Histological observation and pictures of the explants were acquired using optical microscopy (NIKON 90i Fluorescence microscope, NIS Elements Ar software).

2.5. RNA Extraction and Real- time Quantitative PCR (RT- q-PCR)

RNA was extracted as previously described (Pierron et al., 2016c). Briefly, jejunal explants were homogenized in tubes containing plastic beads (MT Biomedicals, Illkirch, France) in 1 mL ExtractAll (Eurobio) using Precellys Evolution tissue homogenizer (Bertin Technologies, Montigny- le-Bretonneux, France). Total RNA was extracted following the manufacturer's recommendations and the concentration and quality of the RNA were assessed using both a Dropsense 96 UV/VIS droplet reader (Trinean, Belgium) and an Agilent 2100 Bioanalyzer (Agilent Technologies Inc., Santa Clara, CA, USA). Their mean (± SD) RNA Integrity Number (RIN) was 6.45 ± 0.26. Two µg of total RNA were reverse transcribed using a High Capacity cDNA Reverse Transcription Kit (Applied Biosystems, Courtaboeuf, France). Primers (Table 1) were designed using the PrimerQuest tool (Integrated DNA Technologies, San Diego, CA, USA) and purchased from Sigma. Real-time PCR assays were performed in duplicate on 5 ng cDNA (5 µL volume reaction per well) in 384-well plates using Power SYBR® Green PCR Master Mix and the Viia7 Real Time PCR System (Applied Biosystems) for data acquisition. Data were analyzed with LinRegPCR software (version 2016.0) and N0 values (starting concentrations) were normalized using hydroxymethylbilane synthase (HMBS) and Beta-2-Microglobulin (B2M) as housekeeping genes. Data are presented in log2 fold change.

2.6. Microarray gene expression studies

Gene expression profiles of the 24 samples (5 replicates per treatment group) were performed at the GeT- TRiX facility (GénoToul, Génopole Toulouse Midi-Pyrénées) using Agilent Sureprint G3 Porcinet 60K_DEC2011 microarrays (8x60K, design 037880) following the manufacturer's instructions, as previously described (Pierron et al. 2016c), Microarray data and experimental details are available in NCBI's Gene Expression Omnibus (Edgar et al., 2002) accessible through GEO Series accession number GSE152763 (https://www.ncbi.nlm.nih.gov/geo/query/acc.cgi?acc=GSE152763).

Functional analysis of the differentially expressed (DE) genes was performed using the Ingenuity Pathway Analysis tool (QIAGEN, Valencia, CA, USA). Only pathways that presented a P value < 0.05 or a $-\log$ P value exceeding 1.30 based on Fisher's exact test are shown.

2.7. Statistical analysis

For cell viability and q-PCR analyses, data are presented as the mean ± standard error of the mean (SEM) and analyzed using Kolmogorov-Smirnov normality test. Analysis of variance (ANOVA) followed by Bonferroni's multiple comparisons test were performed after log transformation of the cell viability results and a paired t-test of the q-PCR data was performed; a p-value < 0.05 was considered significant. The microarray data were analyzed using the Bioconductor packages in R and the limma lmFit function as mentioned in GEO accession GSE152763 and as previously described (Alassane-Kpembi et al., 2017). Data were log2 transformed and normalized using the quantile method, then a correction for multiple testing (False Discovery Rate, FDR) using the Benjamini-Hochberg procedure was applied. Probes with adjusted p values FDR ≤ 0.05 were considered to be differentially expressed between conditions. After hierarchical clustering of the samples, a 1-Pearson correlation coefficient as distance and Ward's criterion for agglomeration were used for the differentially expressed probes.

3. Results

3.1. Cytotoxicity of NX and 3ANX in human intestinal epithelial cells

179 The effects of NX and 3ANX were first compared on proliferating human Caco-2 cells. As shown in
180 Fig. 1, the cell viability measured by ATP quantification decreased significantly from 3 μM and 10 μM
181 with NX and 3ANX, respectively. The longer the exposure to the toxins, the higher the cytotoxicity,
182 with a greater decrease in cell viability (Fig. 1A and 1B). After both 24 h and 48 h of exposure, DON
183 and NX displayed similar cytotoxicity. DON induced a decrease in cell viability starting at 1 μM and
184 significantly different from the control starting at 3 μM; with 3ANX cell viability started to significantly
185 differ from the control at 10 μM. In conclusion, these data showed that the cytotoxicity of NX for the
186 viability of intestinal cells resembled that of DON whereas 3ANX was less cytotoxic.
187
188 3.2 Histological alteration induced by NX and 3ANX in intestinal explants
189 A more complex model was used to complete the analysis. Experiments were performed on whole
190 intestinal tissue, using porcine jejunal explants, a model developed to assess short-term effect of
191 mycotoxins (Alassane-Kpembi et al., 2017; García et al., 2018; Pierron et al., 2016b).
192 The intestinal effects of NX, 3ANX and DON were first compared with histological evaluation (Fig. 2).
193 In comparison to the control, the toxin treated groups (Fig. 2B-D) displayed some interstitial edema and
194 cell debris. Explants treated with DON (Fig. 2C) displayed some loss of villi, and those treated with NX
195 displayed cell vacuolization, a broken epithelial barrier with atrophy and notable loss of villi (Fig. 2B).
196 3ANX-treated explants displayed some cell vacuolization, lymphatic vessel dilation but generally a
197 continuous epithelial barrier (Fig. 2D). In conclusion, histological observations indicated that NX caused
198 greater histological changes to intestinal explants than DON; 3ANX being the least potent.
199
200 3.3 Gene expression profile of intestinal explants exposed to NX, 3ANX and DON
201 A genome wide transcriptomic approach was used to investigate the effects of these new mycotoxins on
202 the intestine at greater depth. Exposure to 10 μM DON, NX and 3ANX resulted in clear modification
203 of the transcriptomic profile of intestinal explants (Fig. 3). The Venn diagram (Fig. 3A) shows that NX
204 induced more differentially expressed genes than DON and 3ANX, with a total of 369 genes (770
205 probes) modulated by NX, 146 genes (315 probes) modulated by DON, and only 55 genes (105 probes)
206 modulated by 3ANX. Principal component analysis of differentially expressed probes separated NX,

DON, 3ANX groups from controls (Fig. 3B). Supervised hierarchical clustering analysis (Fig. 3C) identified two clusters: cluster 1, which included the great majority of 338 genes (736 probes), grouped genes that were up-regulated in response to the toxins, while cluster 2 containing 40 genes (56 probes) grouped genes that were down-regulated in response to DON, NX or 3ANX.

In conclusion, the overall gene expression profile indicated that the three toxins target the intestine and that NX has more impact on intestinal gene expression than DON, 3ANX being the toxin with the least impact.

3.4 Canonical pathways targeted by NX, 3ANX and DON

To further investigate the functional analysis of the differentially expressed genes, we focused on the top genes and pathways modulated by each toxin. The complete list of probes modulated by each toxin is provided in Suppl. Table 1, while Fig. 4 summarizes the top genes and the top pathways modulated by NX, 3ANX and DON.

The genes most differentially expressed by NX were involved in inflammation [Interleukin 1 beta (IL-1B), C-X-C motif chemokine ligand 2 (CXCL2 and GROB), interleukin 22 (IL-22), chemokine ligand 20 (CCL20), interleukin 1 alpha (IL-1A), bradykinin receptor B1 (BDKRB1), selectin E (SELE), tumor necrosis factor alpha-induced protein 3 (TNFAIP3), colony stimulating factor 2 (CSF2), prostaglandin-endoperoxide synthase 2 (PTGS2), chemokine (C-C motif) ligand 4 (CCL4)]; immune response [FOS Like 1 (FOSL1), Cluster of Differentiation 83 (CD83)]; cell proliferation/differentiation/apoptosis and growth [neuron-derived orphan receptor 1 (NOR-1), growth arrest and DNA damage inducible beta (GADD45B), immediate early response 2 (IER2) and 3 (IER3)] (Fig. 4B). The expression level of the majority of these genes was higher upon NX exposure than in the DON and 3ANX treatments. Of note, functional analysis of the 369 genes modulated by NX was pretty similar to the one including only the 231 genes specifically impacted by this toxin (and not modulated by DON or 3ANX, Suppl. Table 2).

Exposure to DON also resulted in increased expression of genes involved in inflammation [IL-1B, IL-22, CCL20, IL-1A, SELE, TNFAIP3, PTGS2, IL-8]; immune response [FOSL1, CD83, bradykinin receptor B2 (BDKRB2), CCR7]; cell proliferation/differentiation/apoptosis and growth [NOR-1, neuregulin 1 (NRG1), calcitonin receptor-stimulating peptide 2 (CRSP-2), ERRF1, AREG,

chromosome 8 open reading frame 4 (CH004), cell migration inducing hyaluronidase 1 (KIAA1199), Rho family GTPase 1 (RND1)].

Genes involved in the same pathways were also overexpressed upon exposure to 3ANX; inflammation [IL-1B, IL-22, IL-1A, TNFAIP3, PTGS2)-, NF-kB inhibitor alpha (NFKBIA), C2 calcium dependent domain containing 4A (C2C4A), phorbol-12-myristate-13-acetate-induced-protein 1 (PMAIP1)]; immune response [CD83, BDKRB2]; cell proliferation/differentiation/apoptosis and growth [NOR-1, neuregulin 1 (NRG1), ERBB receptor feedback inhibitor 1 (ERRF1), amphiregulin (AREG), IER3, cysteine and serine rich nuclear protein 1 (CSRNP1), Sprouty RTK antagonist 2 (SPRY2), interferon related development regulator 1 (IFRD1), polo-like kinase 2 (PLK2), baculoviral IAP repeat containing 3 (BIRC3)]. Over expression of genes involved in inflammation (IL-1A, IL-1B, IL-22, TNFAIP3) and in development/apoptosis (NOR-1) upon NX, 3ANX or DON treatment was confirmed by q-PCR analysis using different biological replicates (Suppl. Fig. 2).

Functional analysis also indicated that the same canonical pathways were modulated by the three toxins (Fig. 4C). TNF receptor-2 (TNFR2), mainly involved in T-reg activity, and TNF receptor-1 (TNFR1) mainly triggering pro-inflammatory activity, as well as several interleukin signaling pathways such as IL-10, IL-17 or IL-6 signaling pathways were among the top canonical pathways targeted by NX, 3ANX and DON. Most of these pathways are involved in the activation of NF-κB and the C-Fos and C-Jun complex (also named AP1).

The first four pathways modulated by NX were further analyzed at gene level (Fig. 5, 6 and Suppl. Fig. 3, 4). The TNRF2 signaling pathway includes 23 genes, of which 14 were modulated by NX with a high $\log_2$FC, ranging from 0.40 to 1.9 (Fig 5). Among these 14 genes, nine were modulated by DON and six by 3ANX, but with a lower $\log_2$FC. Of note, DON and 3ANX did not regulate genes that were not targeted by NX, confirming that NX had a greater impact on the TNRF2 signaling pathway than DON and 3ANX. Analysis of this pathway also showed that five of the NX specific genes (NFkBD, KFkBB, NFkB1, NFkB, TRFA1) belong to signaling pathways regulated by DON and 3ANX. Findings for the IL-10, IL-17 and TNFR1 signaling pathways were similar, with more genes modulated by NX; and with a higher level of up regulation compared to that of DON and 3ANX. As already observed for the TNFR2

pathway, no genes were significantly modulated by DON and/or 3ANX and not modulated by NX in the IL-10, Il-17 and TNFR1 signaling pathways (Fig. 6 and Suppl. Fig. 3, 4).

Of note, the cholecystokinin/gastrin-mediated signaling pathway implicated in the well-known anorexic effect of DON was among the top 20 pathways regulated by DON and 3ANX. This pathway was also highly regulated by NX (-log (p-value) of 5.15, nb of DEG = 10).

Taken together, these results show that more genes in the intestine are modulated by NX than by DON or 3ANX, but that all three toxins modulate the same signaling pathways, particularly inflammatory and immune responses.

4. Discussion

Some populations of *F. graminearum* have been shown to produce the new type A trichothecenes 3ANX and NX, that can occur in *Fusarium*-damaged grains, and prior to this study, available toxicology data were limited. The present study investigated the intestinal toxicity of these newly discovered toxins, using both human intestinal epithelial cells and porcine jejunal explants. DON was included in the study due to its structural similarity with NX and 3ANX.

The effects of NX and 3ANX were first assessed in the well-known human Caco-2 cell model. This enterocyte-like model has the same properties as small intestinal enterocytes and is often used to assess the toxicity of mycotoxins (Alassane-Kpembi et al., 2013; Luo et al., 2021; Sambruy et al., 2001). The cell viability was assessed through the measurement of ATP content. As already described, 48 h exposure to DON decreased ATP content by almost 50% ; which is some how a smaller effect than that the one observed with other viability test (Luo et al. 2021). The equal cytotoxicity of NX and DON observed in this cell line resembled that previously reported in HT29 and HCEC-1CT cells (Varga et al., 2018). An equal effect of NX and DON on protein synthesis inhibition was also observed (Varga et al., 2015). By contrast, 3ANX was less cytotoxic than NX or DON for Caco-2 cells.

The impact of NX and 3ANX was further assessed on intestinal tissue. Due to the difficulties in accessing human intestinal samples, the study was performed on porcine intestinal explants. Pig is a good model for extrapolation to humans, as their digestive physiology is very similar to that of humans (Swindle et al., 2012) and the intestinal explant model has already been used to analyze the intestinal

toxicity of trichothecenes (Alassane-Kpembi et al., 2017; Lucioli et al., 2013; Pierron et al., 2016b). This first assessment of the effect of NX-toxins on tissue morphology revealed intestinal damage including cell vacuolization, cellular debris, a broken epithelial barrier with high atrophy rates and loss of villi. Compared to DON, whose intestinal toxicity is well documented (Bracarense et al., 2020; Pierron et al., 2016), NX was found to be more toxic and 3ANX to be less toxic. The modification and degradation of the intestinal tissues can be due to all the up-regulation of inflammatory genes caused by the toxins as shown by the genome wide analysis (Chen et al., 2018). Given the similarity with what is known for DON, we hypothesize that the damage to intestinal morphology has an impact on barrier function and intestinal absorption (Maresca et al., 2002; Pierron et al., 2016a).

Genome wide analysis confirmed the intestinal impact of the three toxins as well as their potency. The effect of DON has already been described in explant genomic studies but this is the first genome wide analysis performed for NX and 3ANX toxins (Alassane-Kpembi et al., 2018, 2017; Pierron et al., 2016b). Our data show that the three toxins targeted genes implicated in inflammation, immune response, cell proliferation, differentiation, apoptosis, and growth. Several of these genes are linked to NF-kB activity (Hayden and Ghosh, 2014). Using human intestinal cells, Marko's group recently demonstrated that NX activates NF-kB as well as the transcript level of some NF-kB dependent inflammatory cytokines, namely IL8, IL6, IL1beta, and TNFA (Woelflingseder et al., 2020). Our data extend these results to several other genes, notably BCL10, BMP2, CD40, IL1A, IL1R1, PELI1, RELA, TANK, TNF, TNFAIP3.

Transcriptome analysis also showed that NX activates TNFR1, TNFR2 and IL-10 signaling pathways. TNFR1 promotes inflammation through increased production of cytokines such as TNF, IL1B and IL6. By contrast, TNFR2 targets anti-inflammatory effects and promotes stability of regulatory T cells (Treg) lymphocytes (Yang et al., 2018). The anti-inflammatory effect of the IL-10 signaling pathway has also been reported. Thus, the well-known DON paradox, i.e. being both an immunostimulator and an immunosuppressor (Pestka, 2008), may also apply to NX toxins.

Cytotoxicity experiments, histological evaluation, and transcriptional analysis demonstrated reduced toxicity of acetylated NX. To the best of our knowledge, the toxicity of 3ANX has only been studied in *in vitro* translation and was reported to be less potent than NX and DON (Varga et al. 2015). Acetylation

318 is known to reduce the cytotoxicity of trichothecenes. Indeed, 3ADON form of DON, was shown to be
319 less cytotoxic than DON in intestinal proliferating intestinal cells of both human and porcine origin
320 (Alassane-Kpembi et al., 2015, 2013; Payros et al., 2016; Pinton et al., 2012) and to cause milder
321 intestinal histological alteration than DON (Pinton et al., 2012). Similarly, in human Caco-2 cells and
322 in mice splenocytes, 3ADON triggered a lower inflammatory response than DON (Kadota et al., 2013;
323 Wu et al., 2014).
324 Although type A and type B trichothecenes have the same biochemical and cellular targets, substantial
325 differences in the spectrum of toxic effects have been observed *in vivo*. Indeed, the tolerable daily intake
326 of type A trichothecene is lower than that of type B ones (Li et al., 2011; Ohta et al., 1977; SCF, 2002).
327 In jejunal explants, histological and transcriptomic analysis showed that type A trichothecene, NX, is
328 more toxic than its type B counterpart, DON. Although these results need to be confirmed *in vitro*, as
329 the two toxins only differ in the lack of the reactive C8 ketone group, we can hypothesize that this group
330 is involved in the increased toxicity of type A trichothecene.
331

332 **5. Conclusion**

333 NX has recently been shown to occur in *Fusarium* infected grains in US and Canada albeit at lower
334 concentrations, but few people are searching for it using authentic standards or suitable analytical
335 methods. OECD noted the need for continuous monitoring of populations of toxigenic fungi to monitor
336 genetic changes (Hornok 2011). The present study provides a comprehensive view of the toxicological
337 alterations to the intestine caused by the newly discovered toxin, NX, and its acetylated derivative. Using
338 cytotoxicity analysis, histopathological investigations and whole transcriptome profiling, we determined
339 the intestinal toxicity of NX, 3ANX and DON and ranked them in decreasing order: NX>DON>>3ANX.
340 Given the high toxicity of NX, it is important to include this new toxin in the screening of grain samples
341 as well as in the comprehensive risk analysis linked to the presence of trichothecenes in our diet.
342

343

344

Acknowledgement/Funding

We thank Alex Aitken for preparing the pure 3ANX and NX and Ms Goodfellow for the English correction. This research was supported in part by the ANR grant “Newmyco” (ANR-15-CE21-0010), the ANR grant “EmergingMyco” (ANR-18-CE34-0014) and the Ontario Ministry of Food and Agriculture (FS2015-2617 / SF6115).

References

Aitken, A., Miller, J.D., McMullin, D.R., 2019. Isolation, chemical characterization and hydrolysis of the trichothecene 7a-hydroxy, 15-deacetylcalonectrin (3ANX) from *Fusarium graminearum* DAOMC 242077. Tetrahedron Lett. 60, 852-856. https:doi.org10.1016/j.tetlet.2019.02.025

Alassane-Kpembi, I., Gerez, J.R., Cossalter, A.-M., Neves, M., Laffitte, J., Naylies, C., Lippi, Y., Kolf-Clauw, M., Bracarense, A.P.L., Pinton, P., Oswald, I.P., 2017. Intestinal toxicity of the type B trichothecene mycotoxin fusarenon-X: whole transcriptome profiling reveals new signaling pathways. Sci. Rep. 7, 7530. https://doi.org/10.1038/s41598-017-07155-2

Alassane-Kpembi, I., Kolf-Clauw, M., Gauthier, T., Abrami, R., Abiola, F.A., Oswald, I.P., Puel, O., 2013. New insights into mycotoxin mixtures: The toxicity of low doses of Type B trichothecenes on intestinal epithelial cells is synergistic. Toxicol Appl Pharmacol 272, 191–198. https://doi.org/ 10.1016/j.taap.2013.05.023

Alassane-Kpembi, I., Pinton, P., Hupé, J.-F., Neves, M., Lippi, Y., Combes, S., Castex, M., Oswald, I.P., 2018. Saccharomyces cerevisiae Boulardii Reduces the Deoxynivalenol-Induced Alteration of the Intestinal Transcriptome. Toxins (Basel). 10. https://doi.org/10.3390/toxins10050199

Alassane-Kpembi, I., Puel, O., Oswald, I.P., 2015. Toxicological interactions between the mycotoxins deoxynivalenol, nivalenol and their acetylated derivatives in intestinal epithelial cells. Arch. Toxicol. 89, 1337–1346. https://doi.org/10.1007/s00204-014-1309-4

Bracarense, A.P.F.L., Pierron, A., Pinton, P., Gerez, J.R., Schatzmayr, G., Moll, W.-D., Zhou, T., Oswald, I.P., 2020. Reduced toxicity of 3-epi-deoxynivalenol and de-epoxy-deoxynivalenol through deoxynivalenol bacterial biotransformation: *In vivo* analysis in piglets. Food Chem. Toxicol. 140, 111241. https://doi.org/10.1016/j.fct.2020.111241

Chen, L., Deng, H., Cui, H., Fang, J., Zuo, Z., Deng, J., Li, Y., Wang, X., Zhao, L., 2018. Inflammatory responses and inflammation-associated diseases in organs. Oncotarget 9, 7204–7218. https://doi.org/10.18632/oncotarget.23208

Crippin, T., Limay-Rios, V., Renaud, J., Schaafsma, A., Sumarah, M., Miller, J., 2020. *Fusarium graminearum* populations from corn and wheat in Ontario, Canada. World Mycotoxin J 13, 355–366. https://doi.org/10.3920/WMJ2019.2532

Crippin, T., Renaud, J.B., Sumarah, M.W., Miller, J.D., 2019. Comparing genotype and chemotype of *Fusarium graminearum* from cereals in Ontario, Canada. PLoS One 14, e0216735. https://doi.org/10.1371/journal.pone.0216735

Da Silva, E.O., Bracarense, A.P.F.L., Oswald, I.P., 2018. Mycotoxins and oxidative stress: Where are we? World Mycotoxin J. 11, 113–133. https://doi.org/10.3920/WMJ2017.2267

Edgar, R., Domrachev, M., Lash, A.E., 2002. Gene Expression Omnibus: NCBI gene expression and hybridization array data repository. Nucleic Acids Res. 30, 207–210. https://doi.org/10.1093/nar/30.1.207

Gale, L.R., Ward, T.J., Kistler, H.C., 2010. A subset of the newly discovered Northland population of *Fusarium graminearum* from the U.S. does not produce the B-type trichothecenes DON, 15ADON, 3ADON or NIV, in: Proceedings of the National *Fusarium* Head Blight Forum. pp. 48–49.

García, G.R., Payros, D., Pinton, P., Dogi, C.A., Laffitte, J., Neves, M., González Pereyra, M.L., Cavaglieri, L.R., Oswald, I.P., 2018. Intestinal toxicity of deoxynivalenol is limited by *Lactobacillus rhamnosus* RC007 in pig jejunum explants. Arch. Toxicol. 92, 983–993. https://doi.org/10.1007/s00204-017-2083-x

Garreau de Loubresse, N., Prokhorova, I., Holtkamp, W., Rodnina, M. V, Yusupova, G., Yusupov, M., 2014. Structural basis for the inhibition of the eukaryotic ribosome. Nature 513, 517–522. https://doi.org/10.1038/nature13737

Ghareeb, K., Awad, W.A., Böhm, J., Zebeli, Q., 2015. Impacts of the feed contaminant deoxynivalenol on the intestine of monogastric animals: poultry and swine. J. Appl. Toxicol. 35, 327–337. https://doi.org/10.1002/jat.3083

Hayden, M.S., Ghosh, S., 2014. Regulation of NF-κB by TNF family cytokines. Semin. Immunol. 26, 253–266. https://doi.org/10.1016/j.smim.2014.05.004

JEFCA, 2011. Deoxynivalenol. 72nd Joint FAO/WHO Expert Committee on Food Additives and Contaminants. World Heal. Organ. WHO Food A. 791p.

Kadota, T., Furusawa, H., Hirano, S., Tajima, O., Kamata, Y., Sugita-Konishi, Y., 2013. Comparative study of deoxynivalenol, 3-acetyldeoxynivalenol, and 15-acetyldeoxynivalenol on intestinal transport and IL-8 secretion in the human cell line Caco-2. Toxicol. Vitr. 27, 1888–1895. https://doi.org/https://doi.org/10.1016/j.tiv.2013.06.003

Knutsen, H.K., Alexander, J., Barregård, L., Bignami, M., Brüschweiler, B., Ceccatelli, S., Cottrill, B., Dinovi, M., Grasl-Kraupp, B., Hogstrand, C., Hoogenboom, L.R., Nebbia, C.S., Oswald, I.P., Petersen, A., Rose, M., Roudot, A.-C., Schwerdtle, T., Vleminckx, C., Vollmer, G., Wallace, H., De Saeger, S., Eriksen, G.S., Farmer, P., Fremy, J.-M., Gong, Y.Y., Meyer, K., Naegeli, H., Parent-Massin, D., Rietjens, I., van Egmond, H., Altieri, A., Eskola, M., Gergelova, P., Ramos Bordajandi, L., Benkova, B., Dörr, B., Gkrillas, A., Gustavsson, N., van Manen, M., Edler, L., 2017. Risks to human and animal health related to the presence

411 of deoxynivalenol and its acetylated and modified forms in food and feed. EFSA J. 15, e04718.
412 https://doi.org/10.2903/j.efsa.2017.4718
413 Li, Y., Wang, Z., Beier, R.C., Shen, J., De Smet, D., De Saeger, S., Zhang, S., 2011. T-2 toxin, a trichothecene
414 mycotoxin: review of toxicity, metabolism, and analytical methods. J. Agric. Food Chem. 59, 3441–3453.
415 https://doi.org/10.1021/jf200767q
416 Lucioli, J., Pinton, P., Callu, P., Laffitte, J., Grosjean, F., Kolf-Clauw, M., Oswald, I.P., Bracarense, A.P.F.R.L.,
417 2013. The food contaminant deoxynivalenol activates the mitogen activated protein kinases in the intestine:
418 interest of *ex vivo* models as an alternative to *in vivo* experiments. Toxicon 66, 31–36.
419 https://doi.org/10.1016/j.toxicon.2013.01.024
420 Luo, S., Terciolo, C., Neves, M., Puel, S., Naylies, C., Lippi, Y., Pinton, P., Oswald, I.P., 2021. Comparative
421 sensitivity of proliferative and differentiated intestinal epithelial cells to the food contaminant,
422 deoxynivalenol. Environ. Pollut. 277, 116818. https://doi.org/10.1016/j.envpol.2021.116818
423 Maresca, M., Mahfoud, R., Garmy, N., Fantini, J., 2002. The mycotoxin deoxynivalenol affects nutrient absorption
424 in human intestinal epithelial cells. J. Nutr. 132, 2723–2731. https://doi.org/10.1093/jn/132.9.2723
425 Maresca, M., Yahi, N., Younès-Sakr, L., Boyron, M., Caporiccio, B., Fantini, J., 2008. Both direct and indirect
426 effects account for the pro-inflammatory activity of enteropathogenic mycotoxins on the human intestinal
427 epithelium: stimulation of interleukin-8 secretion, potentiation of interleukin-1beta effect and increase in the
428 transepithe. Toxicol. Appl. Pharmacol. 228, 84–92. https://doi.org/10.1016/j.taap.2007.11.013
429 Miller, J.D., 2016. Mycotoxins in food and feed: a challenge for the 21*st* century. Li D-W Biol. microfungi.
430 Springer Int. Publ. Switz. 469–493
431 Ohta, M., Ishii, K., Ueno, Y., 1977. Metabolism of trichothecene mycotoxins. I. Microsomal deacetylation of T-2
432 toxin in animal tissues. J. Biochem. 82, 1591–1598. https://doi.org/10.1093/oxfordjournals.jbchem.a131854
433 Payros, D., Alassane-Kpembi, I., Pierron, A., Loiseau, N., Pinton, P., Oswald, I.P., 2016. Toxicology of
434 deoxynivalenol and its acetylated and modified forms. Arch. Toxicol. 90. https://doi.org/10.1007/s00204-
435 016-1826-4
436 Payros, D., Ménard, S., Laffitte, J., Neves, M., Tremblay-franco, M., Luo, S., 2020. The food contaminant ,
437 deoxynivalenol , modulates the Thelper / Treg balance and increases inflammatory bowel diseases. 90, 2931-
438 2957. https://doi.org/10.1007/s00204-020-02817-z
439 Pestka, J J, 2010. Deoxynivalenol: mechanisms of action, human exposure, and toxicological relevance. Arch.
440 Toxicol. 84, 663–679. https://doi.org/10.1007/s00204-010-0579-8

Pestka, J J, 2010. Deoxynivalenol-induced proinflammatory gene expression: mechanisms and pathological sequelae. Toxins (Basel) 2, 1300–1317. https://doi.org/10.3390/toxins2061300toxins-02-01300 [pii]

Pestka, J J., 2008. Mechanisms of deoxynivalenol-induced gene expression and apoptosis. Food Addit. Contam. Part A, 25, 1128–1140. https://doi.org/10.1080/02652030802056626

Pierron, A., Alassane-Kpembi, I., Oswald, I.P., 2016a. Impact of two mycotoxins deoxynivalenol and fumonisin on pig intestinal health. Porc. Health. Manag. 2, 21. https://doi.org/10.1186/s40813-016-0041-2

Pierron, A., Mimoun, S., Murate, L.S., Loiseau, N., Lippi, Y., Bracarense, A.P.F.L., Schatzmayr, G., He, J.W., Zhou, T., Moll, W.D., Oswald, I.P., 2016b. Microbial biotransformation of DON: Molecular basis for reduced toxicity. Sci. Rep. 6. https://doi.org/10.1038/srep29105

Pierron, A., Mimoun, S., Murate, L.S., Loiseau, N., Lippi, Y., Bracarense, A.-P.F.L., Liaubet, L., Schatzmayr, G., Berthiller, F., Moll, W.-D., Oswald, I.P., 2016c. Intestinal toxicity of the masked mycotoxin deoxynivalenol-3-β-D-glucoside. Arch. Toxicol. 90. https://doi.org/10.1007/s00204-015-1592-8

Pinton, P., Oswald, I.P., 2014. Effect of deoxynivalenol and other type B trichothecenes on the intestine: a review. Toxins (Basel). 6, 1615–1643. https://doi.org/10.3390/toxins6051615

Pinton, P., Tsybulskyy, D., Lucioli, J., Laffitte, J., Callu, P., Lyazhri, F., Grosjean, F., Bracarense, A.P., Kolf-clauw, M., Oswald, I.P., 2012. Toxicity of deoxynivalenol and its acetylated derivatives on the intestine: Differential effects on morphology, barrier function, tight junction proteins, and mitogen-activated protein kinases. Toxicol. Sci. 130, 180–190. https://doi.org/10.1093/toxsci/kfs239

Robert, H., Payros, D., Pinton, P., Théodorou, V., Mercier-Bonin, M., Oswald, I.P., 2017. Impact of mycotoxins on the intestine: are mucus and microbiota new targets? J. Toxicol. Environ. Health. B. Crit. Rev. 20, 249–275. https://doi.org/10.1080/10937404.2017.1326071

Ruan, F., Chen, J.G., Chen, L., Lin, X.T., Zhou, Y., Zhu, K.J., Guo, Y.T., Tan, A.J., 2020. Food Poisoning Caused by Deoxynivalenol at a School in Zhuhai, Guangdong, China, in 2019. Foodborne Pathog. Dis. 17, 429–433. https://doi.org/10.1089/fpd.2019.2710

Sambruy, Y., Ferruzza, S., Ranaldi, G., De Angelis, I., 2001. Intestinal cell culture models: applications in toxicology and pharmacology. Cell Biol. Toxicol. 17, 301–317. https://doi.org/10.1023/a:1012533316609

SCF, 2002. Opinion of the Scientific Committee on Food on *Fusarium* toxins. Part 6: group evaluation of T-2 toxin, HT-2 toxin, nivalenol and deoxynivalenol European Commission.

Swindle, M.M., Makin, A., Herron, A.J., Clubb, F.J.J., Frazier, K.S., 2012. Swine as models in biomedical research and toxicology testing. Vet. Pathol. 49, 344–356. https://doi.org/10.1177/0300985811402846

Varga, E., Wiesenberger, G., Hametner, C., Ward, T.J., Dong, Y., Schofbeck, D., McCormick, S., Broz, K., Stuckler, R., Schuhmacher, R., Krska, R., Kistler, H.C., Berthiller, F., Adam, G., 2015. New tricks of an old enemy: isolates of *Fusarium graminearum* produce a type A trichothecene mycotoxin. Environ. Microbiol. 17, 2588–2600. https://doi.org/10.1111/1462-2920.12718

Varga, E., Wiesenberger, G., Woelflingseder, L., Twaruschek, K., Hametner, C., Vaclavikova, M., Malachova, A., Marko, D., Berthiller, F., Adam, G., 2018. Less-toxic rearrangement products of NX-toxins are formed during storage and food processing. Toxicol. Lett. 284, 205–212. https://doi.org/10.1016/j.toxlet.2017.12.016

Vin, K., Rivière, G., Leconte, S., Cravedi, J.-P., Fremy, J.M., Oswald, I.P., Roudot, A.-C., Vasseur, P., Jean, J., Hulin, M., Sirot, V., 2020. Dietary exposure to mycotoxins in the French infant total diet study. Food Chem. Toxicol. 140, 111301. https://doi.org/10.1016/j.fct.2020.111301

Woelflingseder, L., Del Favero, G., Blazevic, T., Heiss, E.H., Haider, M., Warth, B., Adam, G., Marko, D., 2018. Impact of glutathione modulation on the toxicity of the *Fusarium* mycotoxins deoxynivalenol (DON), NX-3 and butenolide in human liver cells. Toxicol. Lett. 299, 104–117. https://doi.org/10.1016/j.toxlet.2018.09.007

Woelflingseder, L., Gruber, N., Adam, G., Marko, D., 2020. Pro-Inflammatory Effects of NX-3 Toxin Are Comparable to Deoxynivalenol and not Modulated by the Co-Occurring Pro-Oxidant Aurofusarin. Microorganisms. 8, 603. https://doi.org/10.3390/microorganisms8040603

Wu, W., He, K., Zhou, H.-R., Berthiller, F., Adam, G., Sugita-Konishi, Y., Watanabe, M., Krantis, A., Durst, T., Zhang, H., Pestka, J.J., 2014. Effects of oral exposure to naturally-occurring and synthetic deoxynivalenol congeners on proinflammatory cytokine and chemokine mRNA expression in the mouse. Toxicol. Appl. Pharmacol. 278, 107–115. https://doi.org/10.1016/j.taap.2014.04.016

Yang, S., Wang, J., Brand, D.D., Zheng, S.G., 2018. Role of TNF-TNF Receptor 2 Signal in Regulatory T Cells and Its Therapeutic Implications. Front. Immunol. 9, 784. https://doi.org/10.3389/fimmu.2018.00784

You, L., Zhao, Y., Kuca, K., Wang, X., Oleksak, P., Chrienova, Z., Nepovimova, E., Jaćević, V., Wu, Q., Wu, W., 2021. Hypoxia, oxidative stress, and immune evasion: a trinity of the trichothecenes T-2 toxin and deoxynivalenol (DON). Arch. Toxicol. 95, 1899-1915. https://doi.org/10.1007/s00204-021-03030-2

Figures

Table 1- Primer sequences used for RT-qPCR analysis (F: Forward; R: Reverse)

Gene symbol	Gene name	Primer sequence	References
HMBS	Hydroxymethylbilane synthase	F: AGGATGGGCAACTCTACCTG	ENSSSCT00015080370.1
		R: GATGGTGGCCTGCATAGTCT	(this paper)
B2M	Beta-2-Microglobulin	F : CTGCTCTCACTGTCTGG	ENSSSCT00000005170.1
		R : TTCAGGTAATTTGGCTTTCC	(this paper)
IL1B	Interleukin 1 beta	F: ATGCTGAAGGCTCTCCACCTC	NM_214055
		R: TTGTTGCTATCATCTCCTTGCAC	(Bracarense et al., 2020)
NOR-1	Neuron-derived orphan receptor 1	F: CGCCCAGAGATCTTGATTA	ENSSSCG00065057668
		R: GGCTGTGAGAAGGTTGTA	(this paper)
IL22	Interleukin 22	F: CCCAACTCTGATAGATTCCAC	ENSSSCT00000000520.3
		R: GCTGGTCATCACCCTTAAT	(this paper)
IL1A	Interleukin 1 alpha	F: GCCAATGACACAGAAGAAGA	NM_214029
		R: ATGCACTGGTGGTTGATG	(this paper)
TNFAIP3	Tumor necrosis factor, alpha-induced protein 3 (A20)	F: CAACTGGTGTCGAGAAGTGAGG	ENSSSCG00000004154
		R: TCCCCATTCGTTTTCAGTGC	(this paper)

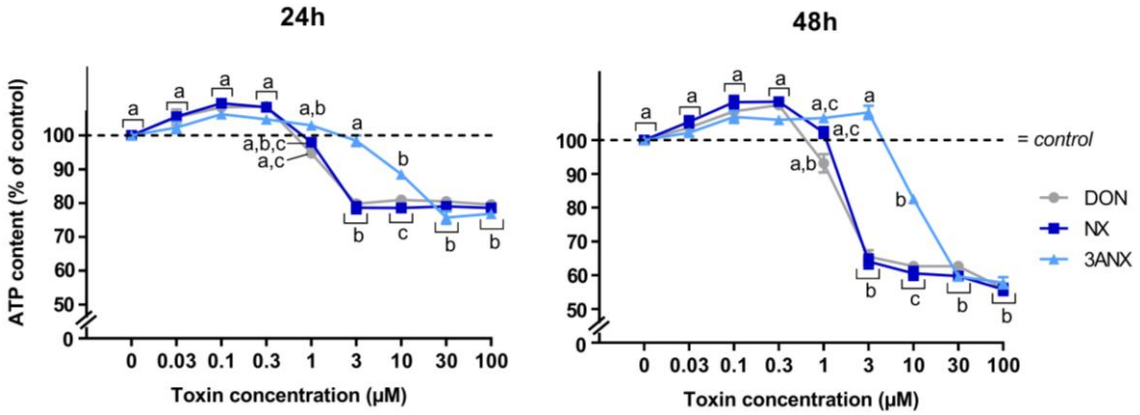

Fig. 1. Toxicity of NX, DON and 3ANX in proliferating Caco-2 cell lines.

Proliferative Caco-2 cells were incubated with increasing concentrations of diluent, NX, DON or 3ANX for 24 h (A) or 48 h (B). Cell viability was evaluated via the CellTiter-Glo Luminescent Cell Viability Assay by measurement of ATP content and is expressed as the % of control cells (dashed line). Results are expressed as the mean ± SEM of 3 independent experiments. Within a panel, means with different letters are statically different, $p < 0.05$ (control being considered as "a").

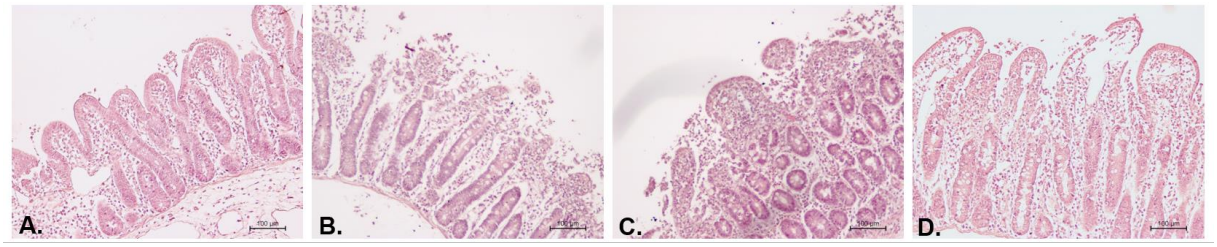

Fig. 2. Toxicity of NX, DON and 3ANX in porcine jejunal explants: histological analysis.

Porcine jejunal explants from one representative animal exposed for 4 h to diluent (A), 10 µM NX (B), 10 µM DON (C) or 10 µM 3ANX (D) and stained with hematoxylin and eosin. *Bar* 100 µm. Control explants: villi with a continuous epithelial barrier (A); NX treated explants: interstitial edema, degradation of epithelial cells, loss of villi and presence of cellular debris (B); DON treated explants: interstitial edema, shortened villi and cell debris (C); 3ANX treated explants: lymphatic vessel dilation and some cell debris with a continuous epithelial barrier (D).

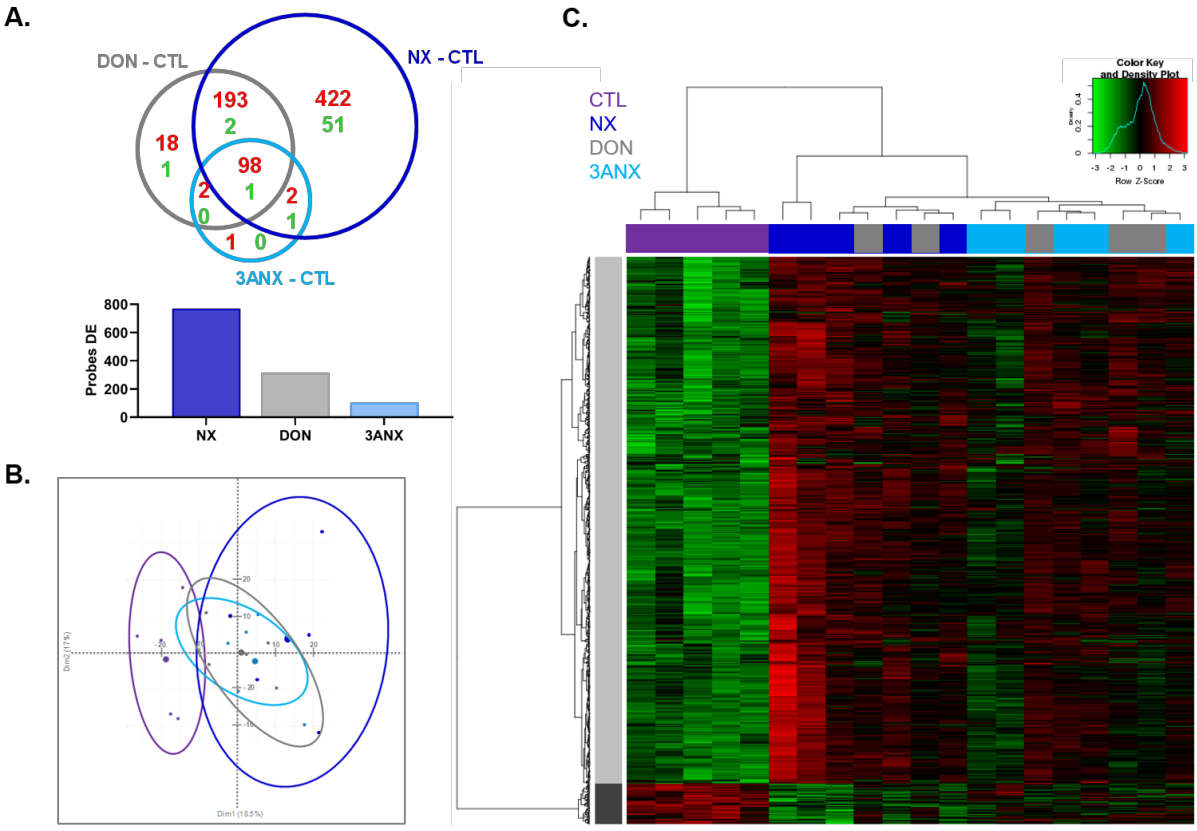

Fig. 3. Gene expression profile of intestinal explants exposed to NX and 3ANX in comparison to DON.

Jejunal explants from 5 animals were exposed for 4 h to diluent (purple), 10 µM NX (dark blue), 3ANX (light

526 blue) or 10 μM DON (grey) and gene expression was analyzed with a 60 K microarray. (A) Venn diagram
527 illustrating the overlaps between probes significantly up- or down-regulated (False Discovery Rate (FDR) p-value
528 ≤ 0.05, Fold Change (FC) ≥ 1) in response to NX, 3ANX or DON (upper panel). Number of differentialy expressed
529 genes in intestinal explants upon exposure to NX, 3ANX and DON (lower panel). (B) Principal component
530 analysis of differential probes between NX, DON, 3ANX and control (with Benjamini-Hochberg (BH) adjusted
531 p-value < 0.05). (C) Heat map representing differentially expressed probes in NX, DON, 3ANX and control
532 explants. Red and green indicate values above and below the mean (average Z-score), respectively. Black indicates
533 values close to the mean.
534
535

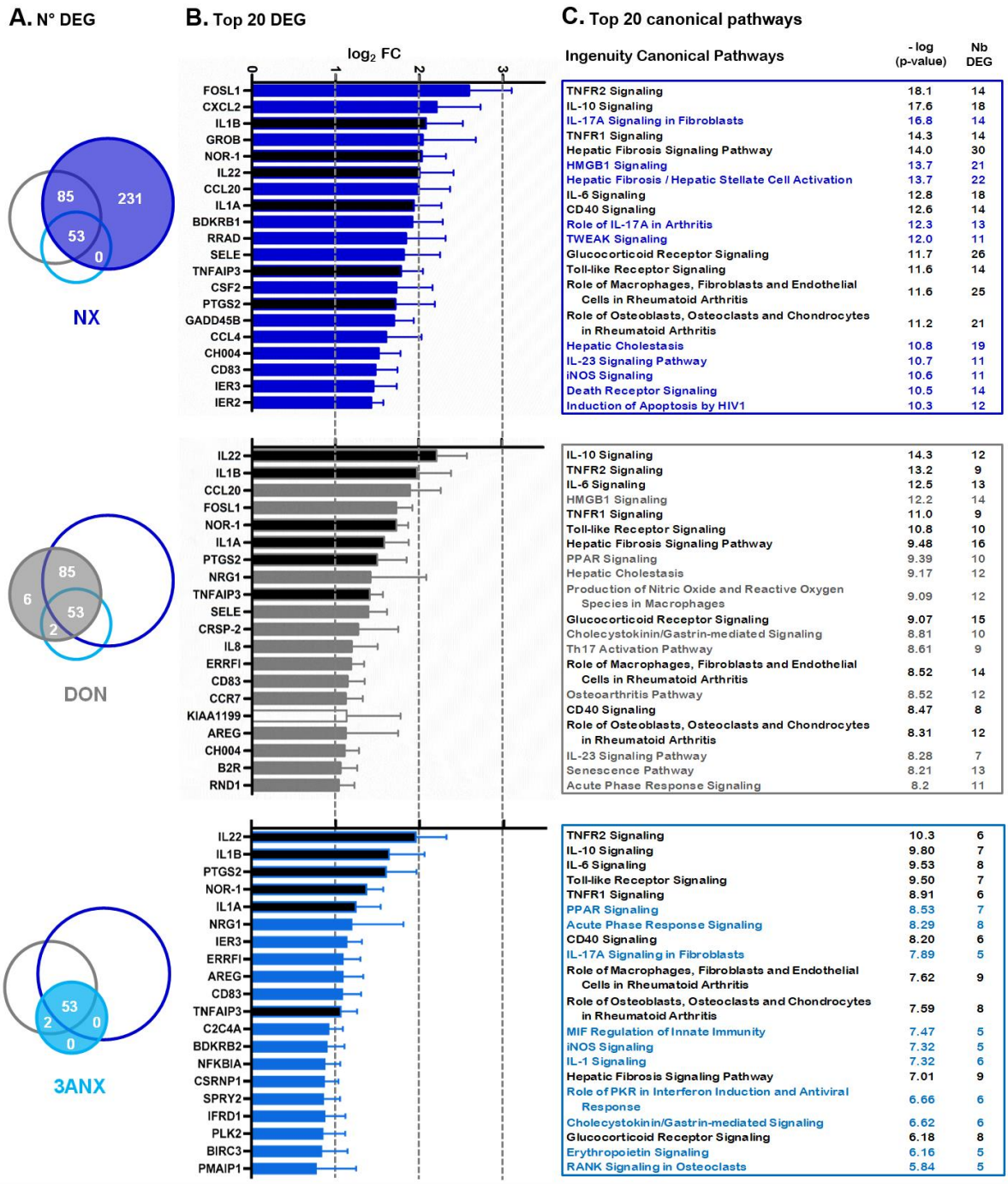

Fig. 4. Comparative analysis of genes and signaling pathways in intestinal explants exposed to NX, 3ANX and DON. Jejunal explants from 5 animals were exposed for 4 h to diluent, 10 µM NX (dark blue), 10 µM DON (grey) or 10 µM 3ANX (light blue). (A) Venn diagram of the number of differentially expressed genes (DEG) in each treatment. (B) Top 20 DEG for each toxin. The closed and open bars indicated up-regulated and down-regulated genes respectively. (C) Top 20 specific canonical pathways significantly modulated by each toxin. The pathways analysis was done using the ingenuity Pathway analysis (IPA) software (Qiagen).

DEG in black bars and canonical pathway in black fonts are common for NX, DON and 3ANX.

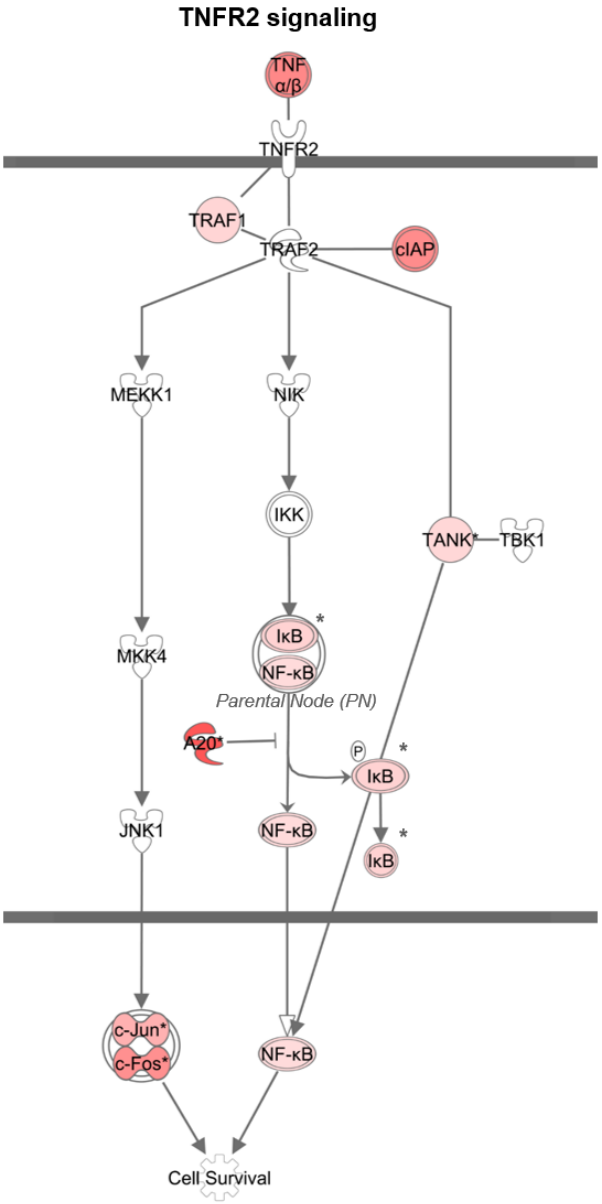

		NX		DON		3ANX	
Symbol	Probe Differentially Expressed	log_2 FoldChange	adjusted p value	log_2 FoldChange	adjusted p value	log_2 FoldChange	adjusted p value
A20	TNFAIP3	1.90	3.29E-05	1.57	1.25E-03	1.19	1.42E-02
c-Fos	FOS	1.25	2.06E-05	0.82	1.53E-03	0.66	2.03E-02
c-Jun	JUN	0.88	2.23E-05	0.67	1.25E-03	0.53	1.42E-02
cIAP	BIRC3	1.30	6.33E-04	0.90	2.30E-02	0.84	4.10E-02
IκB^{PN}	NFKBIE	1.07	2.06E-05	0.87	3.76E-03	0.70	1.42E-02
IκB^{PN}	NKKBIA	1.47	8.37E-05	0.93	7.08E-03	0.88	2.60E-02
*IκB**	NFKBID	0.79	2.67E-03				
IκB^{PN}	NFKBIB	0.50	7.19E-03				
NF-κB^{PN}	NFkB1	0.98	1.92E-02				
NF-κB^{PN}	NFkB2	0.57	6.69E-03	0.48	4.55E-02		
NF-κB^{PN}	RELA	0.40	1.67E-02				
TANK	TANK	0.45	3.76E-02	0.50	3.49E-02		
TNFα/β	TNF-A/B	1.34	1.71E-03	1.04	2.40E-02		
TRAF1	TRAF1	0.48	3.60E-02				

Fig. 5. Differential expression patterns of genes in the TNFR2 signaling pathway in the intestinal tissues exposed to NX, 3ANX or DON

547 The pathways analysis was done using the ingenuity Pathway analysis (IPA) software (Qiagen).

548 Illustration: Expression patterns of genes of the TNFR2 signaling pathway in the jejunal explant exposed to NX.

549 Table: Comparison of probe expression of the genes involved in the TNFR2 signaling pathway in jejunal explants
550 exposed to NX, DON or 3ANX.

551 Red nodes (in the scheme) and red cells (in the table) represent up-regulated genes; darker colors indicate higher
552 gene expression in the differential expression analysis. Uncolored nodes represent genes involved in the signaling
553 pathways that were not differentially expressed by the treatment in the microarray analysis.

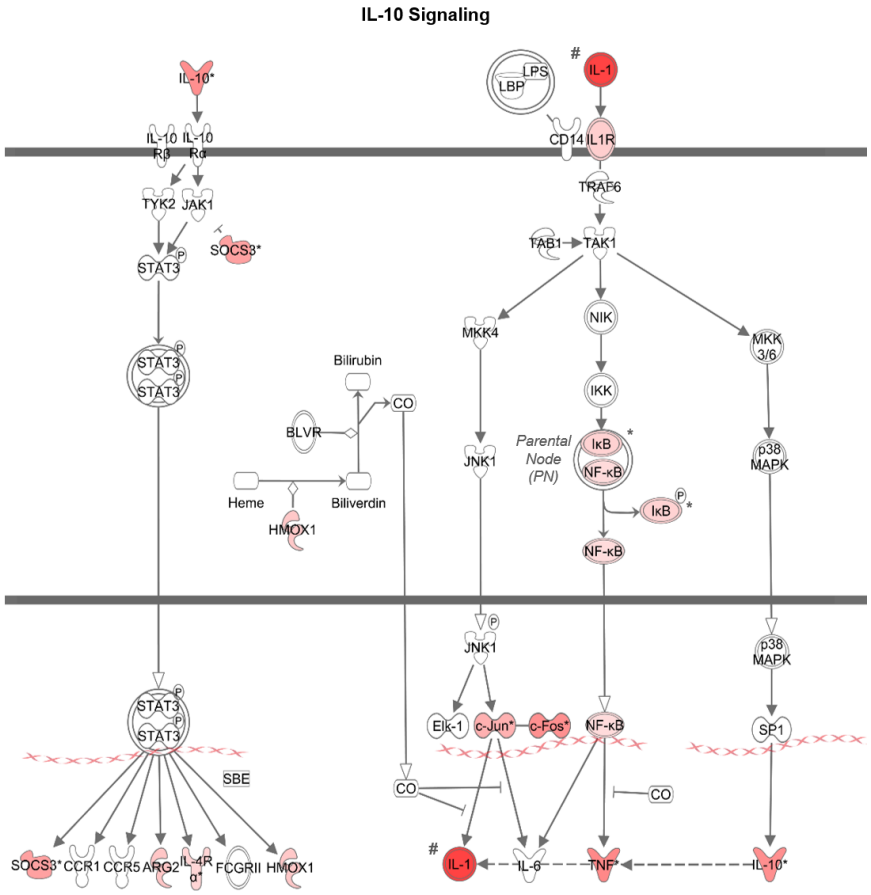

Symbol	Probe Differentially Expressed	NX		DON		3ANX	
		log2 FoldChange	adjusted p value	log2 FoldChange	adjusted p value	log2 FoldChange	adjusted p value
ARG2	ARG2	0.64	2.01E-03	0.49	3.10E-02		
c-Fos	FOS	1.25	2.06E-05	0.82	1.53E-03	0.66	2.03E-02
c-Jun	JUN	0.88	2.23E-05	0.67	1.25E-03	0.53	1.42E-02
HMOX1	HMOX1	0.61	4.03E-02				
IκB^{PN}	NFKBIE	1.07	2.06E-05	0.87	3.76E-03	0.70	1.42E-02
IκB^{PN}	NKKBIA	1.47	8.37E-05	0.93	7.08E-03	0.88	2.60E-02
*IκB**	NFKBID	0.79	2.67E-03				
IκB^{PN}	NFKBIB	0.50	7.19E-03				
IL-1$^{\#}$	IL-1B	2.31	2.22E-04	2.17	2.07E-03	1.70	1.83E-02
IL-1$^{\#}$	IL-1A	2.13	9.30E-05	1.76	1.53E-03	1.39	2.03E-02
IL1R	IL-1RA	0.55	1.13E-02	0.56	2.04E-02		
IL-10	IL10	1.27	5.26E-03	0.70	4.04E-02		
IL-4Rα	IL4R	0.47	2.44E-02				
NF-κB^{PN}	NFkB1	0.98	1.92E-02				
NF-κB^{PN}	NFkB2	0.57	6.69E-03	0.48	4.55E-02		
NF-κB^{PN}	RELA	0.40	1.67E-02				
SOCS3	SOCS3	1.06	4.51E-04	0.68	2.90E-02	0.79	2.60E-02
TNF	TNF	1.34	1.71E-03	1.04	2.40E-02		

Fig. 6. Differential expression patterns of genes of the IL-10 signaling pathway in the intestinal tissue exposed to NX, 3ANX or DON

The pathways analysis was done using the ingenuity Pathway analysis (IPA) software (Qiagen).

Illustration: Expression patterns of genes of the IL-10 signaling pathway in the jejunal explant exposed to NX.

Table: Comparison of probe expression of the genes involved in the IL-10 signaling pathway in jejunal explants exposed to NX, DON or 3ANX. Red nodes (in the scheme) and red cells (in the table) represent up-regulated

genes; darker colors indicate higher gene expression in the differential expression analysis. Uncolored nodes represent genes involved in the signaling pathways that were not differentially expressed by the treatment in the microarray analysis.

Intestinal toxicity of the new discovered type A trichothecenes, NX and 3ANX

CRediT author statement

Alix Pierron: Validation, Formal analysis, Investigation, Writing-original draft, Vizualization. **Manon Neves:** Validation, Formal analysis, Investigation, Writing-original draft. **Sylvie Puel:** Validation, Formal analysis, Investigation. **Yannick Lippi:** Validation, Formal Analysis, Ressources, Data Curation. **Laura Soler:** Writing-review & editing. **J. David Miller:** Ressources, Conceptualization, Funding acquisition. **Isabelle P. Oswald:** Conceptualization, Supervision, Writing-review & editing, Funding acquisition.

Supplementary Figures

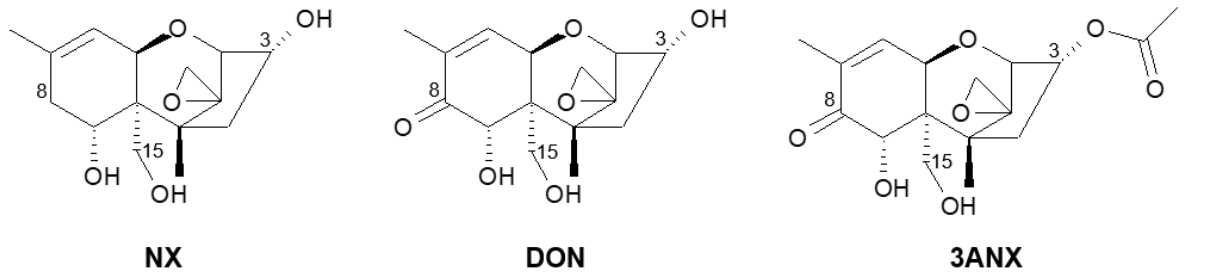

Suppl. Fig. 1. Chemical structures of the three studied toxins

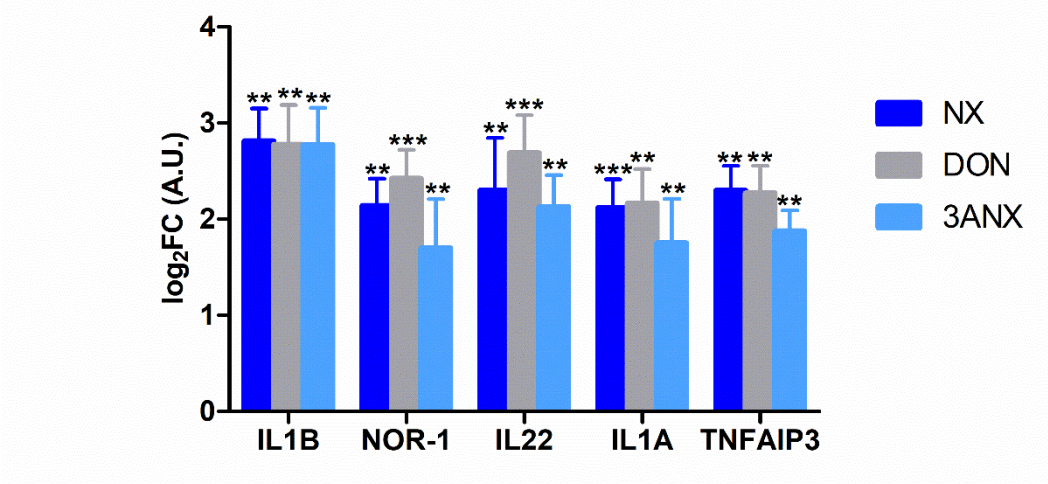

Suppl. Fig. 2. Differentially expressed genes (DEG) induced by the three treatments compared to the control confirmed by q-PCR.

q-PCR of confirmation of representative genes from the same top 20 found in 6 different animals. Results are expressed as mean + SEM of 6 animals, *p < 0.05, **p < 0.01, ***p < 0.001 indicate significant differences from the control condition.

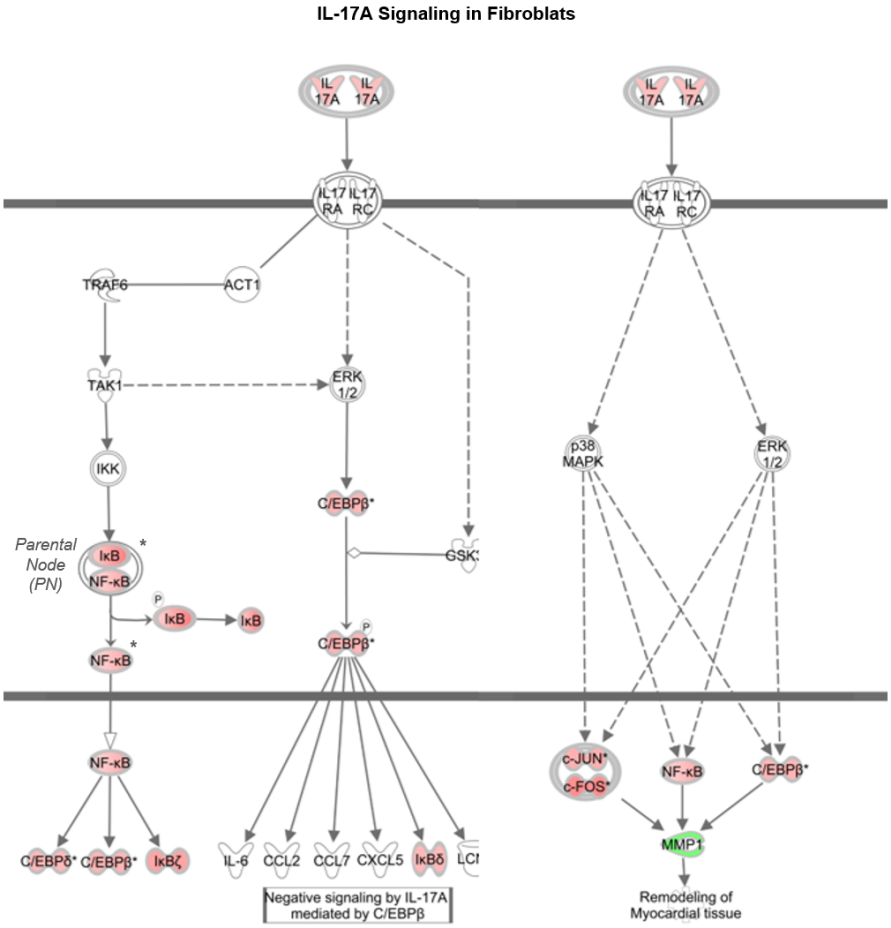

		NX		DON		3ANX	
Symbol	**Probe DE**	**log$_2$FC**	**adj.p value**	**log$_2$FC**	**adj.p value**	**log$_2$FC**	**adj.p value**
c-Fos	FOS	1,25	2,06E-05	0,82	1,53E-03	0,66	2,03E-02
c-Jun	JUN	0,88	2,23E-05	0,67	1,25E-03	0,53	1,42E-02
C/EBPβ	CEBPB	0,83	2,54E-04	0,64	4,86E-03	0,67	1,42E-02
C/EBPδ	CEBPD	0,77	1,25E-02				
IκB^{PN}	NFKBIE	1,07	2,06E-05	0,87	3,76E-03	0,70	1,42E-02
IκB^{PN}	NKKBIA	1,47	8,37E-05	0,93	7,08E-03	0,88	2,60E-02
*IκB**	NFKBID	0,79	2,67E-03				
IκB^{PN}	NFKBIB	0,50	7,19E-03				
IκBζ^{PN}	NFKBIZ	1,01	1,77E-03				
IL17A	IL17A	0,72	4,14E-02				
MMP1	MMP1	-0,43	1,66E-02				
NF-κB^{PN}	NFkB1	0,98	1,92E-02				
NF-κB^{PN}	NFkB2	0,57	6,69E-03	0,48	4,55E-02		
NF-κB^{PN}	RELA	0.40	1.67E-02				

Suppl. Fig. 3. Differential expression patterns of genes of the IL-17A signaling in the fibroblast pathway in the intestinal tissue exposed to NX, 3ANX or DON

The pathways analysis was done using the ingenuity Pathway analysis (IPA) software (Qiagen).

Illustration: Expression patterns of genes of the IL-17A signaling pathway in the jejunal explant exposed to NX.

Table: Comparison of probe expression of the genes involved in the IL-17A signaling pathway in jejunal explants exposed to NX, DON or 3ANX.

Red nodes (in the scheme) and red cells (in the table) represent up-regulated genes; darker colors indicate higher gene expression in the differential expression analysis. Uncolored nodes represent genes involved in the signaling pathways that were not differentially expressed (DE) by the treatment in the microarray analysis.

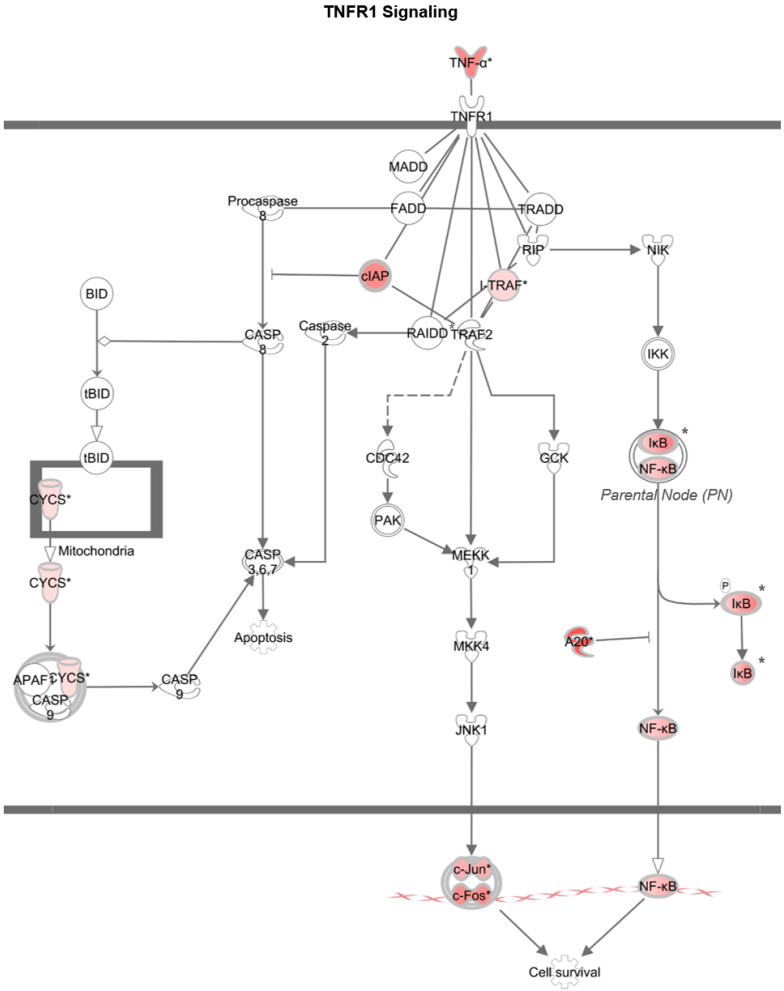

Symbol	Probe Differentially Expressed	NX		DON		3ANX	
		log2 FoldChange	adjusted p value	log2 FoldChange	adjusted p value	log2 FoldChange	adjusted p value
A20	TNFAIP3	1.90	3.29E-05	1.57	1.25E-03	1.19	1.42E-02
c-Fos	FOS	1.25	2.06E-05	0.82	1.53E-03	0.66	2.03E-02
c-Jun	JUN	0.88	2.23E-05	0.67	1.25E-03	0.53	1.42E-02
cIAP	BIRC3	1.30	6.33E-04	0.90	2.30E-02	0.84	4.10E-02
CYCS	CYCS	0.38	3.50E-03				
IκB^{PN}	NFKBIE	1.07	2.06E-05	0.87	3.76E-03	0.70	1.42E-02
IκB^{PN}	NKKBIA	1.47	8.37E-05	0.93	7.08E-03	0.88	2.60E-02
*IκB**	NFKBID	0.79	2.67E-03				
IκB^{PN}	NFKBIB	0.50	7.19E-03				
NF-κB^{PN}	NFkB1	0.98	1.92E-02				
NF-κB^{PN}	NFkB2	0.57	6.69E-03	0.48	4.55E-02		
NF-κB^{PN}	RELA	0.40	1.67E-02				
TANK	TANK	0.45	3.76E-02	0.50	3.49E-02		
TNF	TNF	1.34	1.71E-03	1.04	2.40E-02		

Suppl. Fig. 4. Differential expression patterns of genes of the TNFR1 signaling pathway in the intestinal tissue exposed to NX, 3ANX or DON

The pathways analysis was done using the ingenuity Pathway analysis (IPA) software (Qiagen).

Illustration: Expression patterns of genes of the TNFR1 signaling pathway in the jejunal explant exposed to NX.

Table: Comparison of probe expression of the genes involved in the TNFR1 signaling pathway in jejunal explants exposed to NX, DON or 3ANX.

Red nodes (in the scheme) and red cells (in the table) represent up-regulated genes; darker colors indicate higher gene expression in the differential expression analysis. Uncolored nodes represent genes involved in the signaling pathway that were not differentially expressed (DE) by the treatment in the microarray analysis.

Supp. Table 1. Differentially expressed genes by NX, DON or 3ANX in treated porcine jejunal explants.

Gene expression is expressed in log_2FoldChange (log_2FC).

ProbeName	GeneName	NX		DON		3ANX	
		log_2FC	adjusted p value	log_2FC	adjusted p value	log_2FC	adjusted p value
gi|47523493|ref|NM_214209.1|	ACP5	-0.31689	0.04704				
A_72_P261392	ADAMTS1	0.99358	0.00493	0.87503	0.02574		
O11747	ADAMTS1	1.19254	0.00624	1.03439	0.03578		
A_72_P146551	ADM	0.70269	0.00637				
gi|47523021|ref|NM_214107.1|	ADM	0.72557	0.00680				
O11846	ADM	0.66835	0.02190				
A_72_P150916	AEN	0.43914	0.03674				
A_72_P419794	AEN	0.48594	0.04899				
O702	AKIRIN2	0.30619	0.00711	0.26840	0.03781		
gi|40800179|gb|CK452965.1|CK452965	ALOX12			0.44803	0.04510		
A_72_P190756	AP1S2	-0.25139	0.03564				
A_72_P172586	APTX	-0.21563	0.04149				
A_72_P302799	AREG	1.23468	0.00276	1.19568	0.00731	1.09576	0.03228
gi|47523807|ref|NM_214376.1|	AREG	1.10434	0.00772	1.10452	0.01647		
O10697	AREG	1.17529	0.00809	1.11434	0.02431		
A_72_P440121	AREG	1.09004	0.01030	1.09468	0.02017		
A_72_P709160	ARG2	0.64231	0.00201	0.49173	0.03098		
A_72_P502486	ARID4B	0.34720	0.01571				
O10416	ARID4B	0.34058	0.03002				
A_72_P543827	ARID4B	0.32120	0.03422				
A_72_P132351	ARL5B	0.42734	0.00745				
O9433	ATF3	1.33408	0.00004	1.01442	0.00129	0.77323	0.02027
gi|94438909|gb|EB684318.1|EB684318	ATF3	1.53013	0.00010	1.09288	0.00395		
A_72_P306548	ATF3	0.74609	0.00028	0.50951	0.01410	0.47627	0.04594
A_72_P118076	ATPG	-0.23605	0.04416				
A_72_P299914	B2R	0.90192	0.01179	1.06278	0.00719	0.90629	0.04718
O321	B3GNT2	0.26313	0.02631				
A_72_P137761	BACH1	0.35831	0.01672				
A_72_P334003	BACH2	0.70614	0.04293				
A_72_P490512	BAG3	0.66349	0.00347	0.75236	0.00352	0.69785	0.01727
A_72_P335878	BAG3	0.75918	0.00417	0.83194	0.00458	0.73415	0.02818
O2952	BAG3	0.72007	0.00551	0.76911	0.00715	0.68812	0.03480
gi|115550655|dbj|AK232485.1|	BAG3	0.71776	0.01116	0.77625	0.01350		
A_72_P544072	BAG3	0.65722	0.02570	0.76190	0.01790		
A_72_P332493	BAZ1A	0.56699	0.00443				
A_72_P055921	BAZ1A	0.71791	0.00473				
A_72_P106291	BAZ1A	0.26346	0.02906				
A_72_P082851	BAZ1A	0.30563	0.03040				

O4691	BAZ1A	0.53683	0.03294				
A_72_P643895	BCAS2	0.57142	0.00157				
A_72_P466148	BCAS2	0.52503	0.00688				
A_72_P147081	BCAS2	0.51102	0.00886				
A_72_P573529	BCAS2	0.52312	0.00893				
A_72_P556970	BCAS2	0.45570	0.00995				
A_72_P617083	BCAS2	0.52086	0.01172				
A_72_P560099	BCAS2	0.47292	0.01741				
A_72_P576749	BCAS2	0.50030	0.01839				
A_72_P568274	BCAS2	0.48033	0.02703				
A_72_P567679	BCAS2	0.45534	0.03009				
A_72_P592659	BCAS2	0.45783	0.03294				
A_72_P006241	BCL10	0.40767	0.01072				
A_72_P223297	BCL10	0.43412	0.03039				
A_72_P606828	BCL10	0.41886	0.04681				
A_72_P441349	BCL2A1	1.02188	0.00350	1.02957	0.00717		
A_72_P339363	BCL2A1	0.96553	0.00452	1.00321	0.00719		
A_72_P364933	BCL2L11	0.46682	0.01109				
O9714	BCL2L11	0.40461	0.02544				
A_72_P075251	BCL3	0.48285	0.00087				
gi|115546038|dbj|AK237480.1|	BCL3	0.44157	0.00136				
O13403	BCL3	0.42895	0.00680				
A_72_P245182	BCL6	0.60662	0.01931				
A_72_P774251	BCR	0.43998	0.00333	0.41518	0.01100		
A_72_P107331	BCR	0.35888	0.02677	0.36967	0.04155		
A_72_P077316	BDKRB1	1.92120	0.00587				
A_72_P366043	BHLHE40	0.53111	0.01093				
gi|47523443|ref|NM_214181.1|	BIRC3	1.29679	0.00063	0.90002	0.02302		
A_72_P088296	BIRC3	1.18174	0.00066	0.83327	0.02097	0.84230	0.04104
A_72_P289744	BIRC3	1.00134	0.00128	0.69900	0.03677		
A_72_P692939	BIRC3	0.73344	0.00837	0.64115	0.04340		
A_72_P164316	BMP2	0.53850	0.00298	0.60411	0.00335	0.55554	0.01727
gi|49618793|gb|AY669080.1|	BMP2	0.52901	0.01072	0.56014	0.01527	0.57157	0.02867
A_72_P423809	BMP2	0.48660	0.01477	0.51062	0.02040	0.53728	0.03233
A_72_P764290	BTG1	0.51619	0.00884				
A_72_P155226	BTG1	0.56111	0.01318				
A_72_P733718	BTG1	0.47248	0.01768				
A_72_P035836	BTG1	0.48047	0.03894				
O10201	BTG1	0.47452	0.04923				
gi|90236399|gb|BX666261.2|BX666261	BTG2	1.21348	0.00003	0.86573	0.00153	0.67896	0.02050
A_72_P428459	BTG2	1.21974	0.00008	0.83451	0.00395		
O12642	BTG2	1.18443	0.00009	0.78663	0.00604		
A_72_P232792	BTG2	1.59729	0.00009	0.94635	0.01403		
A_72_P165281	BTG3	0.62530	0.00138				
A_72_P650696	BTG3	0.55078	0.00338				
gi|115546516|dbj|AK234353.1|	BTG3	0.60872	0.00443				

O10241	BTG3	0.57802	0.00899				
A_72_P636792	BTG3	0.54713	0.02082				
O10585	C11orf96	0.87936	0.00826				
A_72_P428974	C11orf96	0.72846	0.03009				
A_72_P125559	C2C4A	1.40211	0.00041	0.82833	0.04689	0.92561	0.04718
A_72_P399928	CA051	0.32763	0.03760				
A_72_P178171	CALCB	0.67939	0.04539	0.86078	0.01825		
A_72_P297794	CCAR1	-0.26810	0.04084				
A_72_P084111	CCD27	0.54122	0.00267				
O1138	CCL20	2.03856	0.00124	1.88070	0.00464		
A_72_P177441	CCL20	1.98370	0.00155	1.90173	0.00461		
gi|66793464|ref|NM_001024589.1|	CCL20	1.97127	0.00171	1.91359	0.00464		
O1921	CCL3L1	1.61656	0.00979				
gi|57527997|ref|NM_001009579.1|	CCL3L1	1.10577	0.01275				
gi|112776193|gb|DB794442.1|DB79...	CCL3L1	1.39777	0.02821				
O1753	CCL4	1.91327	0.00267				
A_72_P223332	CCL4	1.74567	0.00397				
gi|47523285|ref|NM_213779.1|	CCL4	1.16626	0.01600				
A_72_P441594	CCL8	0.94729	0.00164				
A_72_P308453	CCL8	0.94680	0.00169				
gi|29283639|gb|CB477253.1|CB477253	CCL8	0.89559	0.00257				
O4738	CCR4	0.30164	0.03944				
A_72_P223792	CCR7	1.31149	0.00066	1.16495	0.00395		
gi|93205063|ref|NM_001001532.2|	CCR7	1.27001	0.00071	1.12743	0.00426		
A_72_P232617	CD274	0.97140	0.00252	0.83787	0.01620		
gi|68534987|ref|NM_001025221.1|	CD274	0.92748	0.00338	0.85700	0.01350		
A_72_P088376	CD40	0.96885	0.00222				
A_72_P294444	CD40	0.96777	0.00252				
A_72_P124966	CD40	0.91524	0.00378				
gi|47523465|ref|NM_214194.1|	CD40	0.57133	0.00528				
A_72_P544217	CD40	0.75258	0.02272				
A_72_P430119	CD83	1.77695	0.00018	1.39920	0.00363	1.08865	0.04104
gi|14659173|gb|BI184764.1|BI184764	CD83	1.37460	0.00019	0.94949	0.00876		
A_72_P476163	CD83	1.29124	0.00094	1.09841	0.00715		
A_72_P184011	CD93	-0.30463	0.00688				
gi|115554622|dbj|AK237033.1|	CD93	-0.30984	0.02100				
A_72_P715228	CDKN1A	0.78609	0.00336	0.60602	0.04426		
gi|115552646|dbj|AK232851.1|	CDKN1A	0.80307	0.00369	0.63504	0.04155		
A_72_P152936	CDKN1A	0.72213	0.00853				
A_72_P672137	CEBPB	0.80605	0.00009	0.62512	0.00214	0.62745	0.01421
A_72_P642520	CEBPB	0.82575	0.00025	0.63669	0.00486	0.66667	0.01421
A_72_P213602	CEBPB	0.74651	0.00042	0.63290	0.00395	0.58941	0.02027
gi|91176937|gb|DQ450678.1|	CEBPB	0.43183	0.00466	0.36510	0.03294		
A_72_P345453	CEBPD	0.70762	0.00128				
gi|115549724|dbj|AK232003.1|	CEBPD	0.55403	0.00663				
A_72_P474198	CEBPD	0.77439	0.01248				

A_72_P432669	CH004	1.51881	0.00019	1.11320	0.00572		
A_72_P403958	CHAC1	-0.50034	0.01671	-0.48169	0.04155		
gi|59817661|gb|DN123382.1|DN123382	CLEC2B	0.83644	0.01940				
A_72_P444117	COL7A1	-0.29439	0.03944				
O14540	COQ10B	0.72678	0.00128				
A_72_P507873	COQ10B	0.62256	0.01030				
A_72_P419329	COQ10B	0.70300	0.01477				
gi|115553222|dbj|AK233020.1|	CREM	1.01059	0.00171	0.80807	0.01903		
A_72_P256457	CREM	0.81229	0.00360	0.78071	0.01078		
A_72_P081476	CREM	0.95586	0.00397	0.80956	0.02798		
A_72_P280584	CRISPLD1	0.52111	0.00410	0.42791	0.03578	0.60556	0.01421
A_72_P626294	CRK	0.33733	0.00624				
A_72_P142901	CRP	0.32308	0.01754				
A_72_P088266	CRSP-2	1.33406	0.01390	1.27600	0.03760		
gi|50979294|ref|NM_213747.1|	CRSP3	1.41680	0.01672				
O8368	CRY2	0.49740	0.00184	0.36206	0.04019		
O8310	CSF2	1.74436	0.00248				
A_72_P077726	CSF2	1.85024	0.00318				
gi|47523043|ref|NM_214118.1|	CSF2	1.59961	0.00468				
A_72_P351818	CSRNP1	1.29776	0.00008	0.88717	0.00376	0.87513	0.01486
A_72_P197257	CSRNP1	0.29999	0.03934				
O14671	CTGF	0.61533	0.03700				
A_72_P732383	CXCL2	2.31338	0.00303				
A_72_P146411	CXCL2	2.18761	0.00352				
gi|49274638|ref|NM_001001861.1|	CXCL2	2.13582	0.00587				
gi|115546718|dbj|AK237564.1|	CXCR2	0.57978	0.00942	0.74217	0.00363		
A_72_P214947	CXCR2	0.51270	0.02848	0.72863	0.00458		
A_72_P661857	CXCR4	0.60344	0.04293	0.77347	0.01620		
gi|47523297|ref|NM_213773.1|	CXCR4			0.71714	0.00831		
A_72_P599748	CXCR4			0.77174	0.01082		
A_72_P088501	CXCR4			0.69152	0.01620		
A_72_P654023	CYCS	0.38299	0.00350				
A_72_P621955	CYCS	0.31279	0.01538				
A_72_P555705	CYCS	0.32545	0.01625				
A_72_P485031	CYCS	0.31301	0.01768				
A_72_P681213	CYCS	0.29022	0.02715				
A_72_P319303	CYR61	0.85404	0.00133	0.67663	0.01633		
A_72_P688281	CYR61	0.76734	0.00360				
A_72_P580852	CYR61	0.69026	0.01778				
A_72_P552021	CYR61	0.59643	0.04394				
A_72_P016206	DAAM2	-0.28327	0.04648				
A_72_P318768	DCUN1D3	1.02351	0.00126	0.78598	0.01831		
A_72_P157561	DDIT3	0.63223	0.00198				
O11871	DDIT3	0.50821	0.00729	0.47428	0.02479		
A_72_P440751	DDIT3	0.60084	0.02082				
gi|74252282|gb|BW956728.1|BW956728	DDX3X	0.41790	0.02336				

A_72_P751172	DLGAP4	0.20426	0.01668				
O12662	DLL4	0.40020	0.03323				
A_72_P260797	DNAJB1	0.56097	0.00183	0.59929	0.00314	0.46610	0.03480
O11858	DNAJB1	0.55500	0.00281	0.59566	0.00376		
A_72_P268464	DNJB1	0.53391	0.00514	0.59275	0.00486		
A_72_P043881	DPF3	0.25438	0.02772				
A_72_P162971	DUSP1	0.88288	0.00002	0.66892	0.00125	0.51996	0.01421
gi|115553169|dbj|AK232967.1|	DUSP1	0.81423	0.00007	0.65537	0.00125	0.57474	0.01421
O14753	DUSP1	0.73253	0.00009	0.63314	0.00125	0.51869	0.01421
O6367	DUSP2	0.85687	0.02087				
A_72_P254842	DUSP8	0.83189	0.03559				
A_72_P277959	DYN2	0.43390	0.00761				
gi|47523097|ref|NM_213882.1|	EDN1	1.06570	0.00338				
O9936	EDN1	0.94447	0.00587				
A_72_P077871	EDN1	0.97078	0.00899				
A_72_P403598	EGLN3	-0.44330	0.01963				
O11761	EGR1	1.65996	0.00021				
A_72_P305874	EGR1	0.98197	0.00052				
A_72_P006186	EGR1	0.59214	0.00063				
gi|6272255|emb|AJ238156.1|	EGR1	0.79250	0.00092				
O11014	EGR2	0.73373	0.00298	0.54980	0.04741		
A_72_P316053	EGR4	1.41814	0.00346				
O10439	EIF1	0.35702	0.03760				
O13124	ELF3	0.53501	0.03009	0.55129	0.04629		
O13548	ELL	0.69034	0.00478				
A_72_P071596	ELL	0.66064	0.01747				
O12374	ELMSAN1	0.32799	0.03685				
A_72_P379428	ELMSAN1	0.35860	0.03735				
A_72_P311268	ENC1	0.72952	0.00341	0.56390	0.04470		
O8120	ENC1	0.52018	0.03631				
A_72_P330808	ERRFI	1.32648	0.00073	1.19094	0.00395	1.09572	0.02027
A_72_P292674	ETS2	0.45290	0.04149	0.60319	0.01206	0.59858	0.02818
A_72_P033811	ETS2	0.37974	0.04352				
A_72_P155751	ETV3	0.67966	0.01891	0.76196	0.01698		
gi|115547087|dbj|AK231142.1|	EVI2A			0.62747	0.01667		
A_72_P442325	EVI2A			0.52349	0.03677		
A_72_P177461	F3	0.69553	0.01495				
A_72_P056786	F3	0.67246	0.02095				
gi|47523273|ref|NM_213785.1|	F3	0.68138	0.03615				
O9106	FBXO33	0.37299	0.00797				
A_72_P619435	FBXO33	0.36693	0.00808				
A_72_P419204	FBXO33	0.33728	0.04411				
O9934	FILIP1L	0.47301	0.00129	0.45572	0.00376		
A_72_P599488	FILIP1L	0.44868	0.00679	0.54694	0.00376		
A_72_P487105	FILIP1L	0.51157	0.01216	0.55338	0.01481		
A_72_P500905	Flrt3	0.40454	0.03118				

A_72_P251687	FOLR1	-0.29025	0.03330				
A_72_P596714	FOS	1.24367	0.00001	0.79707	0.00125	0.65189	0.01421
A_72_P441284	FOS	1.17260	0.00001	0.79009	0.00125	0.62258	0.01421
gi|115553196|dbj|AK232994.1|	FOS	1.20079	0.00001	0.74271	0.00151	0.64634	0.01421
O9115	FOS	1.24825	0.00002	0.81971	0.00153	0.62193	0.02601
A_72_P205307	FOS	1.22874	0.00002	0.79425	0.00214	0.66060	0.02027
A_72_P670145	FOS	1.08221	0.00002	0.74590	0.00153	0.57380	0.02477
A_72_P414133	FOSB	0.64977	0.01004				
O10489	FOSL1	2.60400	0.00116	1.73501	0.04544		
gi|115551839|dbj|AK236246.1|	FOSL1	2.59398	0.00143				
A_72_P092156	FOXF2	-0.28064	0.04416				
A_72_P102521	FOXL1	-0.32878	0.03767				
A_72_P441344	FOXO1	0.34521	0.03039				
O2815	FRMD4B	0.73433	0.00250				
O8249	GABPB1	0.40487	0.04191				
gi|113205835|ref|NM_001044599.1|	GADD45A	0.83336	0.00427	0.84548	0.00823		
A_72_P146986	GADD45A	0.88431	0.00558	0.87578	0.01337		
O13891	GADD45A	0.81626	0.00587	0.88221	0.00708		
O14595	GADD45B	1.89865	0.00008	1.05018	0.01903		
A_72_P376518	GADD45B	1.62950	0.00014	0.91782	0.02835		
gi|115548802|dbj|AK231760.1|	GADD45B	1.57069	0.00018	0.86836	0.04019		
A_72_P011276	GADD45G	1.24836	0.00008	0.99790	0.00153	0.77733	0.02184
O14936	GADD45G	1.17161	0.00029	0.84053	0.00993		
A_72_P123751	GATA3	0.35417	0.03987				
gi|37798789|gb|CF794226.1|CF794226	GEM	1.33658	0.00174				
A_72_P176381	GEM	1.34219	0.00338				
A_72_P473706	GEM	1.21442	0.00663				
O9699	GPR108	0.26348	0.02962				
gi|115547203|dbj|AK234576.1|	GPR183	0.87244	0.01990	1.00391	0.01544		
A_72_P479120	GPR65	0.80388	0.00053	0.72142	0.00363	0.57638	0.03480
1001448237	GPR65	0.67005	0.00908	0.59527	0.04155		
A_72_P453564	GRAP2	0.25143	0.03518				
A_72_P318383	GRID1	-0.26863	0.04727				
A_72_P401158	GRK5	-0.26946	0.04055				
O8155	GROB	2.05129	0.01790				
gi|74253411|gb|BW984099.1|BW984099	GROB	2.03828	0.01941				
A_72_P616389	GTF2B	0.37400	0.02934				
A_72_P475836	GTF2B	0.31899	0.03009				
A_72_P063756	GTF2B	0.34092	0.04305				
A_72_P544402	H2B2F	0.37924	0.01606				
CUST_342_PI427286967	H3F3A	0.46776	0.00080	0.40979	0.00492		
A_72_P730568	H3F3A	0.44945	0.00097	0.40534	0.00462		
A_72_P742844	H3F3A	0.57324	0.00129				
A_72_P755406	H3F3A	0.51973	0.00138	0.45702	0.00773		
A_72_P724897	H3F3A	0.49783	0.00164	0.43342	0.01027		
A_72_P736180	H3F3A	0.48055	0.00172	0.39559	0.01633		

A_72_P767776	H3F3A	0.48586	0.00174	0.39150	0.01861		
A_72_P757782	H3F3A	0.50822	0.00174	0.46353	0.00760		
A_72_P712893	H3F3A	0.47327	0.00186				
A_72_P750814	H3F3A	0.55071	0.00198	0.40075	0.04177		
A_72_P759235	H3F3A	0.46242	0.00426				
A_72_P744632	H3F3A	0.38084	0.00458	0.36658	0.01350		
A_72_P749783	H3F3A	0.40778	0.00461	0.38419	0.01576		
A_72_P726973	H3F3A	0.49254	0.00528				
A_72_P727673	H3F3A	0.44128	0.00587	0.40416	0.02311		
A_72_P796104	H3F3A	0.43060	0.00859	0.44462	0.01489		
A_72_P753356	H3F3A	0.37544	0.00938	0.35003	0.03163		
A_72_P727423	H3F3A	0.41598	0.01025	0.39316	0.03098		
A_72_P751440	H3F3A	0.49457	0.01085				
A_72_P760267	H3F3A	0.38529	0.01093	0.37564	0.02635		
A_72_P795731	H3F3A	0.35609	0.01544	0.37501	0.02059		
A_72_P735853	H3F3A	0.40874	0.01881				
A_72_P764258	H3F3A	0.37490	0.02095	0.37985	0.03784		
A_72_P749936	H3F3A	0.33772	0.03222				
A_72_P722438	H3F3A	0.37903	0.03425	0.39773	0.04689		
A_72_P721303	H3F3A	0.36338	0.03649				
A_72_P067831	H3F3A	0.29345	0.04648	0.34263	0.03317		
A_72_P177111	H4	0.39173	0.03009				
O4561	HAT1	0.43357	0.00492				
A_72_P178751	HBEGF	1.00144	0.00562				
A_72_P035756	HBEGF	0.75735	0.01389				
O9806	HBEGF	0.72422	0.01567				
A_72_P396743	HERC4	0.35318	0.01390				
gi|115550991|dbj|AK238852.1|	HES1	0.73372	0.00008	0.60130	0.00125	0.43330	0.02601
O14723	HES1	0.56744	0.00023	0.42284	0.00575		
A_72_P292644	HEY1	0.45626	0.01859				
A_72_P285829	HINT3	0.34965	0.01705				
gi|74379699|gb|AJ962883.1|AJ962883	HIVEP1	0.63256	0.01170				
A_72_P002006	HIVEP1	0.59833	0.01501				
A_72_P069996	HMGXB4	0.21699	0.02800				
O13963	HMOX1	0.61423	0.04030				
OTTSUST00000000528	HS71B	0.47844	0.01882	0.47741	0.03771		
A_72_P176131	HSP70	0.57989	0.04149	0.74049	0.01620		
A_72_P088236	HSP70.2	0.38517	0.03118	0.45163	0.02039		
gi|115552968|dbj|AK239554.1|	HSPA8	0.29018	0.02801				
A_72_P061586	HSPA8	0.32422	0.02939				
A_72_P223937	ICAM-1	1.25124	0.00052	0.76106	0.04760		
gi|55742637|ref|NM_213816.1|	ICAM-1	1.25366	0.00137				
A_72_P287144	ICOSLG	0.47551	0.02343				
O8846	ID3	0.38409	0.00688	0.38835	0.01410		
A_72_P225977	ID3	0.39687	0.01052	0.34967	0.04847		
A_72_P066206	IER2	1.42903	0.00001	0.96198	0.00125	0.64191	0.03024

A_72_P025361	IER3	1.74904	0.00027	0.99543	0.04533	1.14026	0.03867
OTTSUST00000000991	IER3	1.60684	0.00080				
A_72_P100451	IER3	1.53593	0.00105				
O4815	IER3	0.92908	0.00617				
A_72_P241737	IER5L	0.41284	0.02800				
A_72_P394573	IFFO2	0.44781	0.00401				
gi|55926204|ref|NM_001007519.1|	IFRD1	1.25768	0.00020	0.98839	0.00376	0.87825	0.02184
A_72_P035786	IFRD1	1.27032	0.00025	0.94753	0.00629	0.84571	0.03241
A_72_P696532	IFRD1	0.86193	0.00052	0.67207	0.00846		
A_72_P108141	IFRD1	0.36457	0.01210				
A_72_P440601	IL10	1.12291	0.00048	0.69527	0.04040		
O12249	IL10	1.25214	0.00174				
gi|47524185|ref|NM_214041.1|	IL10	1.23096	0.00178				
A_72_P185331	IL10	1.26888	0.00526				
O5504	IL17A	0.72100	0.04142				
O1485	IL1A	2.13115	0.00009	1.75567	0.00153	1.38824	0.02027
gi|47522877|ref|NM_214029.1|	IL1A	1.95213	0.00017	1.57900	0.00295	1.27041	0.02818
A_72_P444799	IL1A	1.94651	0.00027	1.58071	0.00376		
A_72_P165276	IL1A	1.72265	0.00029	1.44210	0.00363	1.09154	0.04755
gi|47522925|ref|NM_214055.1|	IL1B	2.30756	0.00022	2.10615	0.00153	1.70428	0.01832
A_72_P441479	IL1B	2.23477	0.00053	2.16472	0.00207	1.58976	0.03586
O8281	IL1B	1.70209	0.00267	1.67923	0.00618		
A_72_P776040	IL1RA	0.55009	0.01126	0.55781	0.02040		
A_72_P186321	IL22	1.98914	0.00020	2.21342	0.00125	1.96000	0.01421
gi|60678608|gb|AY937228.1|	IL22	2.02454	0.00035	2.22139	0.00125	1.97003	0.01421
gi|55742621|ref|NM_214123.1|	IL4	0.77789	0.00026	0.68694	0.00214		
A_72_P146761	IL4	0.79162	0.00171	0.55064	0.04846		
A_72_P088511	IL4R	0.46923	0.00421				
A_72_P003526	IL4R	0.46996	0.02437				
gi|47523123|ref|NM_213867.1|	IL8	1.21275	0.02143				
A_72_P413808	IL8	1.22310	0.02677				
A_72_P232367	IL8	1.18632	0.03115				
CUST_130_PI427286967	IL8	1.13596	0.03503	1.19907	0.04629		
O311	IL8	1.17052	0.03521				
A_72_P442262	INHBA			0.60202	0.03578	0.69658	0.02900
A_72_P442208	INSIG1	0.56179	0.03700	0.59845	0.04630		
A_72_P452692	INTS6	0.43796	0.00421				
A_72_P751922	INTS6	0.38378	0.01268				
A_72_P392088	IPCEF1	0.44786	0.01216				
A_72_P429909	IRAK2	0.65359	0.00157	0.66768	0.00352	0.50415	0.04718
A_72_P516237	IRAK2	0.52911	0.00267	0.51002	0.00725		
gi|115550602|dbj|AK232432.1|	IRF1	1.06996	0.00042				
A_72_P177721	IRF1	1.04562	0.00070				
A_72_P174061	IRF1	0.61713	0.00142				
A_72_P536281	IRF1	0.96135	0.00169				
A_72_P341728	JMJD1C	0.39018	0.03564				

A_72_P178031	JUN	0.88017	0.00002	0.64178	0.00125	0.52486	0.01421
gi|47523101|ref|NM_213880.1|	JUN	0.86262	0.00002	0.67173	0.00125	0.53193	0.01421
A_72_P569634	JUN	0.69362	0.00069	0.54806	0.00999		
O12244	JUN	0.53194	0.00450				
gi|112744780|gb|DB789103.1|DB78...	JUNB	1.05860	0.00017	0.66986	0.01534		
O11588	JUNB	0.81885	0.00171				
gi|26017440|gb|CA779483.1|CA779483	JUND	0.60596	0.00008	0.51778	0.00125	0.36281	0.02818
A_72_P641915	JUND	0.52609	0.00030	0.40236	0.00625		
A_72_P435164	KBTBD2	0.23982	0.03086				
O12836	KDM6B	0.74429	0.00394				
A_72_P314703	KIAA1199	-1.40188	0.00013	-1.13631	0.00214		
A_72_P428929	KLF10	1.62275	0.00008	0.99439	0.00993		
A_72_P567184	KLF10	0.95159	0.00012	0.57792	0.01534		
O10208	KLF10	1.56707	0.00013	0.97653	0.01350		
A_72_P665999	KLF10	0.60580	0.00129	0.44985	0.02439		
A_72_P184666	KLF10	0.62449	0.01778				
O11677	KLF2	0.51435	0.01519				
A_72_P441164	KLF2	0.47310	0.01556				
A_72_P584261	KLF4	0.58307	0.00531				
A_72_P584816	KLF4	0.57844	0.00587				
A_72_P577783	KLF4	0.53329	0.00761				
A_72_P672762	KLF4	0.37166	0.02631				
gi|72535179|ref|NM_001031782.1|	KLF4	0.38921	0.03564				
A_72_P303164	KLF4	0.34645	0.04229				
gi|110007346|gb|DQ682407.1|	KLF5	0.29498	0.03425				
A_72_P217292	KLF6	0.63847	0.00245				
A_72_P251132	KLF6	0.69972	0.00269				
A_72_P607553	KLF6	0.59070	0.00406				
O8141	KLF6	0.55574	0.00663	0.47354	0.04155		
A_72_P262797	KLF6	0.53776	0.00679	0.45301	0.04557		
A_72_P118106	KLF6	0.53287	0.01556				
A_72_P088486	KLF7	0.45096	0.02366				
A_72_P634101	KLF7	0.35284	0.03564				
A_72_P008541	KLF7	0.41244	0.03564				
O8199	KLF7	0.33777	0.04826				
gi|47523857|ref|NM_214402.1|	LIF	1.25003	0.02017				
O4949	LITAF	0.34991	0.04777				
A_72_P158981	LITAF	0.33532	0.04879				
A_72_P548861	LMNA	0.27141	0.03157				
A_72_P302689	LMNA	0.20745	0.04826				
A_72_P068316	LOC100050031	0.55010	0.01159	0.57269	0.01766		
A_72_P241047	LOC100151774	-0.22043	0.03346				
A_72_P222172	LOC100151957	0.42223	0.00772	0.36208	0.04557		
A_72_P246487	LOC100152725	0.27951	0.01171	0.28715	0.01927		
A_72_P038896	LOC100153143	-0.29645	0.02851				
A_72_P033861	LOC100153522	-0.21155	0.01990				

A_72_P014381	LOC100153947	-0.24516	0.01901				
A_72_P372593	LOC100155620	0.49754	0.04202				
A_72_P169591	LOC100156540	-0.32558	0.03987				
A_72_P246752	LOC100156697	0.40535	0.00232				
A_72_P008201	LOC100157062	1.23638	0.03201				
A_72_P157521	LOC100157454	-0.35922	0.00300	-0.31062	0.01831	-0.34014	0.02518
A_72_P199902	LOC100158011	-0.28919	0.01859				
A_72_P299199	LOC100158021	-0.26649	0.02252				
A_72_P363083	LOC101909268	-0.31908	0.02156				
A_72_P297519	LOC102167231	0.33560	0.04100				
A_72_P317548	LOC461758	0.29930	0.01339				
gi|72535195|ref|NM_001031791.1|	LOC595121	0.32655	0.00528				
A_72_P242237	LOC595121	0.43304	0.01571				
A_72_P165711	LOC595121	0.24963	0.04826				
A_72_P039421	LOC735483	0.76482	0.00777				
A_72_P054436	LOC781336	0.30327	0.03086				
O7967	LONRF1	0.35687	0.01941				
O907	M3K8	0.49810	0.01323				
A_72_P260627	M3K8	0.76110	0.01403				
A_72_P022356	MARCH3	0.82237	0.02824				
O8831	MARCKSL1	0.94375	0.01806				
O5799	MAX	-0.24008	0.02659				
O9280	MBTPS1	-0.23398	0.04509				
A_72_P423944	MCL1	0.53749	0.00041	0.32650	0.04040		
A_72_P226568	MCL1	0.59694	0.00119	0.49495	0.01041		
A_72_P475140	MCL1	0.59332	0.00269	0.46665	0.03262		
A_72_P554706	MCL1	0.58224	0.00520				
A_72_P592644	MCL1	0.49884	0.01802				
gi|47523779|ref|NM_214361.1|	MCL1	0.46857	0.04051				
A_72_P039326	MED20	0.35444	0.01596				
A_72_P356133	MEFV	0.60802	0.04218				
A_72_P442223	MEST	0.86279	0.00531	0.88630	0.00941		
O12643	MEST	0.53867	0.03614	0.63099	0.02427		
A_72_P517687	MEST			0.49414	0.04592		
A_72_P636782	MEX3C	0.48510	0.04017				
A_72_P339208	MGEA5	-0.24863	0.04652				
A_72_P140941	MIDN	0.35346	0.00127				
A_72_P413508	MMP1	-0.42537	0.01662				
O12996	MOB3C	0.69031	0.00318				
O11111	MT2A	0.48649	0.02135				
gi|1827468|dbj|AB000794.1|	MT2A	0.45138	0.03793				
A_72_P592239	MYC	1.11774	0.01093				
A_72_P557580	MYC	1.11512	0.01123				
A_72_P165831	MYC	1.04809	0.01318				
O12961	MYC	1.02145	0.01668				
gi|52346219|ref|NM_001005154.1|	MYC	1.01145	0.02437				

A_72_P191761	N4BP2L1	0.31551	0.03944					
gi|77404427|ref|NM_001031793.2|	NAMPT	0.73709	0.00448					
A_72_P035446	NAMPT	0.69252	0.01802					
A_72_P440276	NAMPT	0.63130	0.03040					
A_72_P229097	NCOA7	0.67073	0.00948					
A_72_P092651	NCOA7	0.68831	0.02437					
A_72_P003616	NDEL1	0.55844	0.00222	0.54067	0.00611			
O9539	NDEL1	0.56643	0.00728	0.52950	0.02439			
A_72_P678820	NEDD9	0.57962	0.00038	0.47255	0.00462	0.44473	0.02027	
A_72_P552156	NEDD9	0.60090	0.00643	0.55754	0.02302			
A_72_P670582	NEDD9	0.53813	0.00727	0.51634	0.02039	0.63742	0.01556	
A_72_P243527	NEDD9	0.54593	0.01110	0.49237	0.04470			
A_72_P006571	NFAC1	0.51329	0.00281					
O10462	NFIL3	0.85226	0.00182			0.69479	0.03867	
A_72_P487453	NFIL3	0.80820	0.00269	0.65308	0.02685	0.72165	0.03024	
A_72_P314698	NFIL3	0.46030	0.01013			0.55080	0.01727	
A_72_P278054	NFKB1	0.84524	0.01141					
O12055	NFKB1	0.95619	0.01596					
A_72_P146316	NFKB1	0.87769	0.01705					
gi|115312275|ref|NM_001048232.1|	NFKB1	0.98035	0.01925					
gi|115554668|dbj|AK237079.1|	NFKB2	0.56478	0.00612					
A_72_P291514	NFKB2	0.57162	0.00669	0.48112	0.04551			
O9695	NFKB2	0.46657	0.02177					
A_72_P342398	NFKBIA	1.47442	0.00008	0.92852	0.00708	0.88148	0.02601	
A_72_P600868	NFKBIA	1.39572	0.00023	0.79849	0.03953			
O12168	NFKBIA	1.37711	0.00032	0.86079	0.02835			
A_72_P165846	NFKBIA	1.26628	0.00033	0.83918	0.01888			
gi|52346211|ref|NM_001005150.1|	NFKBIA	1.30937	0.00041	0.84487	0.02690			
A_72_P209997	NFKBIA	1.35137	0.00051	0.82801	0.04470			
O7164	NFKBIB	0.50110	0.00719					
A_72_P132521	NFKBIB	0.47091	0.00899					
O11433	NFKBID	0.78652	0.00267					
A_72_P118631	NFKBIE	1.06870	0.00002	0.72752	0.00136	0.69727	0.01421	
O9827	NFKBIE	1.05142	0.00013	0.80980	0.00337	0.66752	0.02818	
A_72_P508686	NFKBIE	1.02231	0.00036	0.86742	0.00376			
A_72_P542623	NFKBIE	0.59545	0.00342					
gi|74255355|gb|BW978515.1|BW978515	NFKBIE	0.51261	0.00560	0.45655	0.02672			
A_72_P333618	NFKBIZ	1.01379	0.00177					
O5248	NGDN	0.32220	0.01656					
A_72_P072231	NHP2L1	0.30483	0.01941					
gi|11501414|gb|BF441322.1|BF441322	NINJ1	0.50919	0.00338	0.40006	0.03852			
A_72_P593734	NKRF	0.40460	0.00624	0.33375	0.04793			
A_72_P413628	NOR-1	1.13965	0.00002	0.93349	0.00125	0.68307	0.01421	
A_72_P637266	NOR-1	2.28485	0.00008	1.94037	0.00125	1.60255	0.01421	
A_72_P574174	NOR-1	2.21614	0.00008	1.90213	0.00125	1.54299	0.01421	
A_72_P302674	NOR-1	2.26291	0.00009	1.95770	0.00125	1.53824	0.01727	

gi|47523565|ref|NM_214247.1|	NOR-1	2.27227	0.00013	1.93882	0.00153	1.50671	0.02184
gi|18534829|gb|BM484501.1|BM484501	NR4A1	1.13292	0.00008	0.97916	0.00125	0.74381	0.01727
O8955	NR4A1	1.12570	0.00026	0.73845	0.01667		
gi|15038571|gb|BI345282.1|BI345282	NR4A2	1.07338	0.00016	0.89626	0.00207	0.64399	0.04104
A_72_P408573	NR4A2	0.87637	0.00017	0.75419	0.00178	0.63182	0.01727
O12486	NR4A2	1.04157	0.00018	0.95232	0.00141	0.66505	0.03283
A_72_P008081	Nr4a3	1.06577	0.00008	0.77617	0.00334	0.60465	0.03586
A_72_P296444	NRG1	1.06701	0.00409	1.39801	0.00153	1.18291	0.01486
gi|59811438|gb|DN117178.1|DN117178	NRG1	1.03116	0.00587	1.44940	0.00136	1.21368	0.01421
A_72_P205272	NUAK2	0.88842	0.00046	0.79688	0.00337		
A_72_P259537	NUAK2	0.89512	0.00248	0.80053	0.01247		
A_72_P487508	NUDT18	0.29815	0.04143				
A_72_P499549	NUP153	0.51316	0.01915				
gi|115550157|dbj|AK235636.1|	ODC1	0.41800	0.01593	0.42281	0.02891		
CUST_500_PI427286967	ODC1	0.38482	0.02156	0.43881	0.01730		
O9222	OTUD1	0.92661	0.00296				
A_72_P323578	PARD6B	0.43090	0.03040				
A_72_P348738	PARP16	0.47493	0.04912				
A_72_P036711	PARPT	0.74555	0.00164	0.59519	0.01855		
A_72_P228302	PDE12			0.22652	0.04868		
A_72_P560384	PDE4B	0.68009	0.00886				
A_72_P440971	PDE4B	0.69408	0.01407	0.68779	0.02985		
A_72_P058356	PDE4B	0.54735	0.04575				
A_72_P443195	PDK4	0.36326	0.01922				
A_72_P188651	PELI1	0.46013	0.04411				
O12878	PER1	0.39906	0.01399				
O12205	PFKFB3	0.94840	0.00109				
O12014	PHACTR1	0.48883	0.00679	0.50361	0.01206		
A_72_P337823	PHACTR1			0.49551	0.01620		
A_72_P050676	PHF11	0.30753	0.02909				
O9244	PHLDA1	0.67181	0.02991				
A_72_P319533	PHLDA2	0.75259	0.00145	0.71588	0.00462	0.62956	0.02818
A_72_P193412	PIM1	0.65190	0.00301				
A_72_P691414	PINX1	0.32046	0.00269				
A_72_P427479	PLEKHA8	-0.22360	0.03844				
A_72_P088596	PLIN2	0.56024	0.03676				
A_72_P268494	PLK2	1.01320	0.00179	0.83018	0.01739	0.87194	0.02818
O10770	PLK2	0.94220	0.00298	0.82390	0.01706	0.83846	0.03283
A_72_P303319	PMAIP1	1.07435	0.00018	1.06970	0.00125	0.77695	0.01727
gi|47523385|ref|NM_214147.1|	PMAIP1	1.10143	0.00021	1.06006	0.00125	0.84014	0.01539
A_72_P444508	PMAIP1	0.70663	0.00250	0.75479	0.00372		
A_72_P195002	PNRC1	0.58386	0.00145				
A_72_P675044	PNRC1	0.58609	0.00548				
A_72_P593749	PNRC1	0.61944	0.00595				
A_72_P596979	PNRC1	0.56186	0.00622				
A_72_P705135	PNRC1	0.44649	0.01915				

A_72_P500305	PNRC1	0.48185	0.02852				
O13367	PPP1R10	0.50767	0.00587				
A_72_P404043	PPP1R15A	1.16503	0.00017	0.92028	0.00346	0.74616	0.03024
A_72_P108796	PPP2R2A	0.31872	0.02032	0.35031	0.02059		
A_72_P128051	PRDM1	0.67287	0.00385	0.76044	0.00376	0.68729	0.02027
A_72_P491930	PRDM1	0.53024	0.02751	0.72422	0.00575	0.59765	0.04755
O7626	PRDM1	0.46795	0.03009	0.69190	0.00376	0.56006	0.03586
A_72_P031371	PRDM1			0.65454	0.00458		
A_72_P322513	PROCR	1.09643	0.00680				
A_72_P591519	PROCR	0.94389	0.01013				
A_72_P336123	PROCR	0.94535	0.02057				
A_72_P416293	PRR2	0.41663	0.00663				
gi|115553405|dbj|AK236608.1|	PRR2	0.22466	0.04826				
gi|47523707|ref|NM_214321.1|	PTGS2	1.73925	0.00473	1.54475	0.02357	1.65776	0.03233
O10093	PTGS2	1.68564	0.00587	1.47037	0.03262	1.56090	0.04455
A_72_P443218	PTGS2	1.69918	0.00617	1.50607	0.03055	1.57212	0.04718
A_72_P302784	PTGS2	1.74707	0.00637	1.49761	0.03934	1.65435	0.04104
A_72_P506963	PTPN2	0.25467	0.04899				
A_72_P055491	PTPRA	-0.21623	0.02817				
A_72_P022341	PUR1	0.43653	0.04879				
A_72_P490030	R3HCC1L	0.37828	0.00137	0.30363	0.01576		
A_72_P190496	RAB21	0.33461	0.02265				
O9083	RABAC1	-0.23133	0.02380				
A_72_P190776	RABGEF1	0.33489	0.02787				
A_72_P069541	RASGEF1B	0.52265	0.00157	0.45561	0.00962		
A_72_P404973	RCAN1	1.35514	0.03697				
A_72_P337088	REL	0.82855	0.01297				
O9322	RELA	0.39878	0.01672				
O3543	RGS1	0.93674	0.00303	1.03990	0.00357		
A_72_P413538	RGS1	0.99759	0.00303	1.08480	0.00376		
gi|5823136|gb|AF139837.1|AF139837	RGS1	1.00520	0.00328	0.99618	0.00725		
A_72_P165546	RGS16	0.62993	0.03164				
gi|113205849|ref|NM_001044600.1|	RGS2	1.00033	0.00012	0.81164	0.00207		
A_72_P088221	RGS2	0.93965	0.00042	0.80293	0.00376		
A_72_P057121	RGS2	0.84487	0.00046	0.72772	0.00376		
A_72_P175291	RHOB	0.53369	0.00035	0.42016	0.00572		
A_72_P630896	RHOB	0.62382	0.00053	0.43519	0.01971		
A_72_P624308	RHOB	0.49769	0.00062	0.35506	0.01831		
A_72_P336448	RHOB	0.60570	0.00109	0.46852	0.01620		
gi|115548954|dbj|AK235357.1|	RHOB	0.64610	0.00133	0.46087	0.03338		
A_72_P566619	RHOB	0.67206	0.00163	0.50190	0.02955		
A_72_P506395	RHOB	0.60518	0.00269	0.44895	0.04630		
A_72_P643885	RHOB	0.51760	0.01004				
A_72_P620824	RHOB	0.47536	0.01508				
A_72_P623634	RHOB	0.41238	0.02677				
O7861	RIOK2			0.28289	0.02374		

A_72_P247442	RIPK2	0.60401	0.02154				
A_72_P032256	RLF	0.34205	0.02726				
gi|15036106|gb|BI342817.1|BI342817	RND1	1.18775	0.00023	0.98925	0.00326		
O8646	RND1	1.15985	0.00129	1.09728	0.00426		
A_72_P035816	RND3	0.81142	0.00023	0.61037	0.00545		
O12382	RND3	0.64794	0.00066	0.47136	0.01706	0.49793	0.02818
A_72_P306333	RND3	0.74171	0.00156				
A_72_P367373	RNF19B	0.47575	0.01959				
A_72_P157941	RNF6	0.62076	0.03009				
O11805	RRAD	1.90518	0.00335				
A_72_P141121	RRAD	1.75513	0.00360				
A_72_P109831	RRAD	1.87482	0.00719				
O14634	SAG			0.35650	0.03098		
O11453	SCLT1	0.36489	0.04727				
A_72_P440056	SELE	1.88201	0.00171	1.40014	0.03262		
gi|47523601|ref|NM_214268.1|	SELE	1.78274	0.00337				
O3768	SELE	1.81640	0.00354				
A_72_P035596	SELE	1.79641	0.00447				
A_72_P203022	SERTAD3	0.47042	0.00066				
O10149	SGK1	0.52171	0.00089				
A_72_P236482	SGK1	0.50913	0.00210	0.38774	0.03301		
A_72_P153871	SH2B2	0.33074	0.00624				
A_72_P262117	SH2D2A	0.47942	0.01217	0.43612	0.04557		
O5944	SH2D2A	0.44933	0.03714				
O9514	SH3BP2	0.34033	0.00688				
O12507	SIK3	0.28670	0.03589				
O1571	SKIL	0.58837	0.00037	0.45890	0.00629		
O11118	SLC25A33	0.41032	0.01741	0.40991	0.03455		
A_72_P150231	SLC25A33	0.46955	0.02994				
A_72_P020856	SLC30A9	-0.20783	0.04787				
CUST_166_PI427286967	SLC35B2	0.43445	0.01925				
A_72_P303729	SLC35B2	0.41451	0.03226				
A_72_P495085	SLC46A2	0.39939	0.02734				
A_72_P146611	SMAD3	0.34529	0.04265				
A_72_P089786	SMNDC1	0.39508	0.00859				
A_72_P004801	SMOX			0.44993	0.01825	0.52860	0.01727
O12282	SMOX					0.51606	0.03586
O11214	SNAI1	0.81281	0.00137	0.72428	0.00708		
A_72_P290864	SNIP1	0.29500	0.03692				
A_72_P257347	SNRK	0.28545	0.03157				
O9277	SOCS3	1.00610	0.00031	0.63281	0.02633	0.70514	0.02818
A_72_P367438	SOCS3	1.05650	0.00045	0.68393	0.02898	0.79249	0.02601
A_72_P319193	SOX17	0.43883	0.01887				
O13061	SOX4	0.47205	0.00157	0.45298	0.00462	0.44697	0.01727
A_72_P404508	SOX4	0.40943	0.04923				
gi|47523169|ref|NM_213843.1|	SOX9	0.47315	0.00027	0.36436	0.00535	0.31351	0.03480

A_72_P146931	SOX9	0.59814	0.01066				
A_72_P288694	SPRY1	0.46094	0.03330				
O12145	SPRY2	0.86613	0.00531	0.85401	0.01330	0.86175	0.02818
A_72_P373863	SPSB1	0.41905	0.01738				
A_72_P060256	SPTY2D1	0.36828	0.01046	0.33526	0.04019		
A_72_P021496	SPTY2D1	0.38019	0.03425				
A_72_P286564	ST17A	0.38966	0.02800				
A_72_P305704	STAT4	0.47076	0.01464	0.45724	0.03541		
A_72_P189401	STX11	1.15361	0.00138				
A_72_P503867	STX11	1.63026	0.00153				
O640	STX11	1.46313	0.00338				
A_72_P378508	SYS1	0.32530	0.02939				
A_72_P709805	TAGAP	0.28207	0.03357				
gi|115552257|dbj|AK230566.1|	TANK	0.42691	0.02103	0.42120	0.04470		
A_72_P080821	TANK	0.44974	0.03760	0.50417	0.03492		
A_72_P340593	TBC1D4	0.59580	0.04899	0.68246	0.03999		
A_72_P433344	TBC1D4			0.45187	0.03897		
O7931	TBPL1	0.31865	0.00909				
A_72_P589634	TBX3	0.41738	0.00269	0.44432	0.00376	0.47842	0.01421
A_72_P499269	TBX3	0.49372	0.00337	0.45546	0.01350	0.49285	0.02027
A_72_P041196	TBX3	0.45926	0.01390	0.51942	0.01206	0.47936	0.04228
A_72_P637494	TBX3	0.42986	0.03944	0.51503	0.02302		
O11729	TBX3			0.33673	0.01693		
A_72_P488239	TBX3			0.28893	0.04791		
A_72_P142606	TCAM1	0.42112	0.02801				
A_72_P117871	TIMP1	0.68111	0.01941				
A_72_P223927	TIMP1	0.92588	0.02994				
O10493	TIMP1	0.92456	0.03236				
A_72_P106826	TNAP2	1.06555	0.00679				
OTTSUST00000000652	TNF	1.34317	0.00171	1.04074	0.02397		
O8075	TNF	1.14766	0.00203	0.85699	0.03677		
A_72_P211447	TNF	1.08579	0.00210	0.81516	0.03650		
A_72_P146356	TNF	1.00045	0.00289	0.84452	0.02059		
A_72_P538206	TNF	0.51634	0.00454	0.48757	0.01542		
gi|84124390|gb|CV870430.1|CV870430	TNFAIP2	0.83717	0.01803				
A_72_P100136	TNFAIP3	1.90124	0.00003	1.57326	0.00125	1.19255	0.01421
A_72_P374863	TNFAIP3	1.71729	0.00008	1.36365	0.00153	1.04109	0.02421
A_72_P320813	TNFAIP3	1.70328	0.00008	1.31977	0.00207	1.04936	0.02477
gi|74259135|gb|BW982295.1|BW982295	TNFAIP3	1.81444	0.00009	1.39371	0.00245	1.00266	0.04718
A_72_P063236	TNFRSF12A	0.77660	0.00826				
gi|52351393|gb|AY609823.1|	TNFRSF12A	0.69418	0.01756				
O6355	TNFRSF12A	0.68521	0.03521				
gi|40426989|gb|BP436922.1|BP436922	TNFSF15	0.47084	0.03009	0.48133	0.04839		
O3158	TNN	-0.69988	0.03955				
A_72_P195417	TNR18			0.59065	0.04923		
A_72_P131876	TNRC6B	-0.24349	0.03462				

O14192	TOPORS	0.38483	0.00350				
A_72_P162066	TOPORS	0.35598	0.04058				
A_72_P115716	TR10D	0.44969	0.03119				
A_72_P420514	TRA2B	0.31333	0.00610				
A_72_P328513	TRA2B	0.26996	0.03118				
A_72_P088081	TRA2B	0.32925	0.04191				
A_72_P569614	TRA2B	0.27146	0.04923				
gi|15032692|gb|BI339409.1|BI339409	TRAF1	0.47569	0.03595				
A_72_P317388	TSC22D1	0.38476	0.04493	0.43288	0.04040		
A_72_P486304	TSC22D2	0.49493	0.00384	0.46695	0.01337		
A_72_P401653	TSC22D2	0.59927	0.01022				
A_72_P003771	TTI2	0.28597	0.03564				
O9185	TUBB4B	0.22100	0.04293				
A_72_P612897	TXNIP	0.43647	0.00500				
A_72_P562489	TXNIP	0.38026	0.00638	0.33537	0.03279		
A_72_P146541	TXNIP	0.42651	0.00713				
A_72_P574349	TXNIP	0.39771	0.01247				
A_72_P673176	TXNIP	0.34213	0.01754				
A_72_P585156	TXNIP	0.30837	0.04084				
A_72_P657299	UAP1	0.46639	0.03767				
O5637	UBALD1	0.43480	0.00826				
A_72_P073056	UBALD1	0.38104	0.01280				
A_72_P529525	UBB	0.35386	0.02484				
A_72_P326078	UBB	0.36203	0.03700				
O10707	UBC	0.37911	0.02136	0.38181	0.04011		
A_72_P114776	UBIQ	-0.26851	0.04416				
A_72_P094676	UGCG	0.37484	0.01778				
A_72_P174051	UPP1	-0.29693	0.04293				
A_72_P245402	USP54	0.44296	0.01213	0.40712	0.04267		
A_72_P575659	V1AR	0.52417	0.04512				
gi|47522703|ref|NM_213891.1|	VCAM1	0.94470	0.02544				
O11774	VCAM1	0.53664	0.02693				
A_72_P293294	VWF	-0.33329	0.03767				
A_72_P007731	ZBTB10	1.00901	0.00053				
A_72_P024886	ZBTB10	1.09931	0.00171				
A_72_P128421	ZBTB10	0.96869	0.00292				
A_72_P553876	ZBTB10	0.88486	0.01474				
A_72_P473857	ZBTB10	0.71432	0.04293				
A_72_P257407	ZBTB11	0.54671	0.00277				
O10928	ZBTB2	0.54359	0.00030	0.44135	0.00395		
A_72_P296334	ZBTB2	0.84136	0.00042	0.58096	0.01739		
A_72_P659488	ZFAND5	0.77357	0.00017	0.67289	0.00154	0.63957	0.01421
A_72_P638042	ZFAND5	0.73815	0.00044	0.66754	0.00314	0.56831	0.02184
A_72_P599678	ZFAND5	0.51157	0.00109	0.37203	0.02427		
A_72_P660923	ZFAND5	0.69831	0.00127	0.67262	0.00376	0.57343	0.02818
A_72_P369638	ZFAND5	0.51066	0.00129	0.45113	0.00708		

A_72_P653310	ZFAND5	0.57310	0.00171					
A_72_P563124	ZFAND5	0.58742	0.00267					
A_72_P570994	ZFAND5	0.56233	0.00338					
A_72_P539158	ZFAND5	0.62096	0.00341	0.60775	0.00862			
A_72_P582317	ZFAND5	0.47273	0.00414					
A_72_P584076	ZFAND5	0.56564	0.00436					
A_72_P592919	ZFAND5	0.57438	0.00663					
A_72_P602666	ZFP36L1	0.47556	0.01201					
A_72_P585515	ZFP36L1	0.49397	0.02566					
A_72_P530580	ZIC4	0.77454	0.00008					
A_72_P193062	ZNF295	0.53661	0.00521	0.44751	0.03929			
A_72_P021206	ZNF441	0.32988	0.03330					
O4628	ZNF622	0.34851	0.01928					
A_72_P371233	ZNF622	0.36306	0.04017					
A_72_P194697	ZRANB2	-0.29659	0.02925					
O5694	ZSWIM6	0.37509	0.00442					
A_72_P294394	ZSWM4	0.41928	0.03767					
A_72_P122192	ZXDC	0.27904	0.02920					
A_72_P234322		0.78673	0.00091	0.65205	0.00839			
A_72_P228962		0.38356	0.00157					
A_72_P184106		0.93677	0.00191					
A_72_P343913		0.97822	0.00232					
A_72_P010216		0.93497	0.00298					
A_72_P208722		0.50100	0.00409	0.46577	0.01544			
A_72_P366288		0.78195	0.00528					
A_72_P338613		0.42702	0.00658	0.36329	0.04155			
A_72_P008841		0.80056	0.00679	0.74547	0.02357			
A_72_P224472		1.54421	0.00761	1.38634	0.03423	1.51223	0.03916	
A_72_P234402		0.52246	0.00809					
A_72_P266732		-0.34279	0.00916					
A_72_P178526		0.64833	0.01004	0.87568	0.00276	0.66997	0.03480	
A_72_P128976		0.61492	0.01059					
A_72_P265047		0.33355	0.01126					
A_72_P094051		-0.71071	0.01158					
A_72_P311448		0.62012	0.01249					
A_72_P420899		-0.39593	0.01477					
A_72_P415453		-0.25478	0.01606					
A_72_P367953		-0.37201	0.01637					
A_72_P113766		-0.33669	0.01754					
A_72_P144291		0.59722	0.01920					
A_72_P192327		-0.30864	0.01941					
A_72_P201592		0.77570	0.02271					
A_72_P081221		-0.82082	0.02428					
A_72_P344708		0.42555	0.02555					
A_72_P139876		0.33801	0.02787					
A_72_P252477		-0.24706	0.02962			-0.28985	0.04063	

A_72_P327633		0.60906	0.03194			
A_72_P386583		-0.28397	0.03425			
A_72_P339938		0.26629	0.03425			
A_72_P022856		-0.35812	0.03463			
O3515		-0.31184	0.03496			
A_72_P159811		0.25273	0.03632	0.33503	0.01036	
A_72_P318278		0.27188	0.03887			
A_72_P215157		0.62709	0.04149			
A_72_P011986		0.54486	0.04512			
A_72_P008286		-0.23293	0.04559			
A_72_P060236		0.43802	0.04601			
A_72_P429984		0.37181	0.04727			
A_72_P363878		-0.29433	0.04826			
A_72_P364133		0.46421	0.04899			
A_72_P020476		-0.28177	0.04974			
A_72_P023291				-0.34222	0.01790	
A_72_P276809				0.70701	0.02431	
A_72_P000156				0.30039	0.03784	

39

40

Supp. Table 2. Comparative analysis of signaling pathways modulated by NX. Jejunal explants from 5 animals were exposed for 4 h to diluent, 10 µM NX. Comparative analysis of the top 20 specific canonical pathways from the specific 231 DEG only modulated by NX (black fonts) and the 369 DEG modulated by NX (including the ones also modulated by DON and/or 3ANX).

Ingenuity Canonical Pathways	-log (p-value)	
	DEG NX only	DEG NX
IL-17A Signaling in Fibroblasts	9.09E00	1.68E01
TWEAK Signaling	7.67E00	1.20E01
Small Cell Lung Cancer Signaling	5.84E00	9.53E00
HER-2 Signaling in Breast Cancer	5.46E00	2.18E01
Hepatic Fibrosis / Hepatic Stellate Cell Activation	5.24E00	1.37E01
TNFR2 Signaling	5.19E00	1.80E01
Role of IL-17A in Arthritis	5.1E00	1.23E01
4-1BB Signaling in T Lymphocytes	5.06E00	9.40E00
Hepatic Fibrosis Signaling Pathway	4.91E00	1.40E01
Death Receptor Signaling	4.79E00	1.05E01
Induction of Apoptosis by HIV1	4.76E00	1.03E01
CD40 Signaling	4.69E00	1.26E01
April Mediated Signaling	4.59E00	9.94E00
Apoptosis Signaling	4.57E00	9.94E00
B Cell Activating Factor Signaling	4.54E00	9.70E00
Role of IL-17F in Allergic Inflammatory Airway Diseases	4.44E00	5.75E00
iNOS Signaling	4.35E00	1.06E01
Angiopoietin Signaling	4.34E00	5.97E00
TNFR1 Signaling	4.14E00	1.43E01
Lymphotoxin β Receptor Signaling	4.02E00	6.15E00